

# Influence of initial soil moisture in a Regional Climate Model study over West Africa. Part 2: Impact on the climate extremes.

Brahima KONÉ<sup>1</sup>, Arona DIEDHIOU<sup>1, 2</sup>, Adama Diawara<sup>1</sup>, Sandrine Anquetin<sup>2</sup>, N'datchoh Evelyne Touré<sup>1</sup>, Adama Bamba<sup>1</sup> and Arsene Toka Koba<sup>1</sup>

<sup>1</sup>LAPAMF, Université Félix Houphouët Boigny, Abidjan, Côte d'Ivoire

<sup>2</sup>Univ. Grenoble Alpes, IRD, CNRS, Grenoble INP, IGE, F-38000 Grenoble, France

*Correspondence to:* Arona DIEDHIOU (aronadiedhiou@ird.fr)

## **Abstract.**

The influence of the initial soil moisture conditions on extreme climate extreme over West Africa was investigated using the fourth generation of Regional Climate Model version 4 (non-hydrostatic) coupled to the version 4.5 of the Community Land Model (RegCM4-CLM4.5) at 25 km spatial resolution. Sensitivity studies were performed for five years (2001-2005), with initial soil moisture conditions prescribed on June 1 and simulations performed over four months (120 days) from June to September (JJAS). The Results were presented for two extreme years 2003 (above normal precipitation year) and 2004 (below normal precipitation year) to estimate the impact limits of internal forcing of initial soil moisture on the new non-hydrostatic dynamical core of RegCM4. We initialized the control runs with the reanalysis soil moisture of the European Centre Meteorological Weather Forecast's reanalysis of the 20th century data (ERA20C), while for the dry and wet experiments, we initialized the soil moisture at the maximum and minimum value over West Africa studied domain, respectively. The impact on extreme precipitation indices of the initial soil moisture, especially over the central Sahel, is linear; that is, dry (wet) experiments decrease (increase) precipitation extreme indices only for precipitation indices related to the number of precipitation events, not for those related to the event intensity. Initial soil moisture conditions unequally affect the daily minimum and maximum temperatures. A stronger impact is found on the maximum temperature than the minimum temperature. Over the entire West African domain, wet (dry) experiments cause a decrease (increase) in maximum temperature. The impact of initial soil moisture conditions on the indices related to the minimum temperature (TN<sub>x</sub> and TN<sub>n</sub> indices) is linear only for TN<sub>x</sub> index over central Sahel, that is, dry (wet)

32 experiments cause an increase (a decrease) in the TNx index. The performance of RegCM4-  
33 CLM4.5 in simulating the ten extreme rainfall and temperature indices used in this study are  
34 also highlighted.

35

## 36 **1 Introduction**

37 West Africa experienced large rainfall variability during the late 1960s. This variability often  
38 leads to flooding events, severe drought, and regional heatwaves, which have major  
39 economic, environmental, and societal impacts (Easterling et al., 2000; Larsen, 2003). In  
40 recent years, climate extremes have attracted much interest because they are expected to occur  
41 more frequently (International Panel on Climate Change (IPCC), 2012) than changes in the  
42 mean climate. Yan and Yang (2000) showed that for many cases, the extreme climate changes  
43 were five to ten times greater than climate mean change. Many key factors or physical  
44 mechanisms could be the cause of the increase in climate extremes (Nicholson, 1980; Le  
45 Barbé et al., 2002), such as the effect of increasing greenhouse gases in the atmosphere on the  
46 intensification of hot extremes (IPCC, 2007), sea surface temperature (SST) anomalies  
47 (Fontaine and Janicot 1996; Folland et al., 1986), and land surface conditions (Philippon et  
48 al., 2005; Nicholson (2000)). In addition, smaller-scale physical processes, including the  
49 interactions of land–atmosphere coupling, can lead to changes in climate extremes. For the  
50 European summer, the influence of soil moisture on land–atmosphere coupling using a  
51 regional climate model and focused on the extremes and trends in precipitation and  
52 temperature have been studied by Jaeger and Seneviratne (2011). For extreme temperatures,  
53 their studies have shown that interactions of soil moisture and climate have a significant  
54 impact, while for extreme precipitation, they only influence the frequency of wet days. Over  
55 Asia, Liu et al. (2014) studied the impact on subsequent precipitation and temperature of soil  
56 moisture anomalies using a regional climate model. They showed that wet (dry) experiences  
57 decrease (increase) the hot extremes, decrease (increase) the drought extremes, and increase  
58 (decrease) the cold extremes in a zone with strong soil moisture–atmospheric coupling.  
59 However, none of these studies examined the impacts of the initial soil moisture conditions on  
60 subsequent climate extremes using a regional climate model over West Africa. **In part 1, the  
61 influence of initial soil moisture on the climate mean was based on a performance assessment  
62 of the Regional Climate Model coupled with the complex Community Land Model  
63 (RegCM4-CLM4.5) performed by Koné et al. (2018), where the ability of the model to**

64 reproduce the climate mean has been validated. In Part 2, before starting to study the  
65 influence of initial soil moisture on climate extremes, it was necessary to assess the  
66 performance of RegCM4-CLM4.5 in simulating the ten (10) indices of temperature and  
67 precipitation extremes used in this study. This has never been done before in West Africa with  
68 this version of RegCM with a non-hydrostatical scheme; therefore, we separated the work in  
69 two parts, a first one assessing the ability of the model to simulate the climate extreme  
70 indices, and a second one investigating how and what is the time limit of the effect of initial  
71 soil moisture condition on the magnitude or duration of these climate extremes. The  
72 manuscript is organized as follows: Section 2 describes the RegCM4 model, the experimental  
73 design, and the methodology used in this study; Section 3 presents results of the two parts of  
74 the work and Section 4 documents the main conclusions.

## 75 **2. Model, experimental design and methodology**

### 76 **2.1 Model description and numerical experiment**

77 The fourth generation of the Regional Climate Model (RegCM4) of the International Centre  
78 for Theoretical Physics (ICTP) is used in this study. Since this version, physical  
79 representations have been subject to a continuous process of implementation and  
80 development. The release used in this study was RegCM4.7. The non-hydrostatic dynamical  
81 core of the MM5 (Mesoscale Model version 5, Grell et al., 1994) was ported to RegCM4  
82 while maintaining the existing hydrostatic core. RegCM4 is a limited-area model using a  
83 vertical grid sigma hydrostatic pressure coordinate and a horizontal grid of the Arakawa B-  
84 grid (Giorgi et al., 2012). The radiation scheme is from the NCAR-CCM3 (National Center  
85 for Atmospheric Research and the Community Climate Model Version 3) (Kiehl et al., 1996),  
86 and the aerosol representation is from Zakey et al. (2006) and Solmon et al. (2006). The large-  
87 scale precipitation scheme used in this study is from Pal et al. (2000); the moisture scheme is  
88 called the SUBgrid EXplicit moisture scheme (SUBEX), which considers the sub-grid  
89 variability in clouds. The accretion and evaporation processes for stable precipitation are from  
90 Sundqvist et al. (1989). The sensible heat and water vapour in the planetary boundary layer  
91 over land and ocean, as well as the turbulent transport of momentum, is reported by Holtslag  
92 et al. (1990). The heat and moisture and momentum of ocean surface fluxes are from Zeng et  
93 al. (1998). Convective precipitation and land surface processes in RegCM4.7 are represented  
94 in several options. Based on Koné et al. (2018), the convective scheme of Emanuel (1991) is  
95 used. The parameterization of land surface processes is from CLM4.5 (Oleson et al., 2013). In

96 each grid cell of CLM4.5, there are sixteen different plant functional types and ten soil layers  
97 (Lawrence et al., 2011; Wang et al., 2016). The integration of RegCM4 over the West African  
98 domain is shown in Fig. 1 with eighteen vertical levels and 25 km of horizontal resolution  
99 ( $182 \times 114$  grid points; from  $20^{\circ}\text{W}$ – $20^{\circ}\text{E}$  and  $5^{\circ}\text{S}$ – $21^{\circ}\text{N}$ ). The European Centre for Medium-  
100 Range Weather Forecasts reanalysis (EIN75; Uppala et al., 2008; Simmons et al., 2007)  
101 provides the initial and boundary conditions. The sea surface temperatures (SSTs) are derived  
102 from the National Oceanic and Atmosphere Administration optimal interpolation weekly  
103 (NOAA; OI\_WK) (Reynolds et al., 1996). The topography is derived from the United States  
104 Geological Survey (USGS) Global Multi-resolution Terrain Elevation Data (GMTED;  
105 Danielson et al., 2011) at a spatial resolution of 30 arc-s, which is an update of the Global  
106 Land Cover Characterization (GTOPO; Loveland et al., 2000) dataset.

107 The initial soil moisture sensitivity does not exceed four months (Hong and Pan., 2000; Kim  
108 and Hong, 2006). (Hong and Pan., 2000; Kim and Hong, 2006). As mentioned in Part I, we  
109 performed sensitivity studies on the initial soil moisture conditions over the West African  
110 domain for June–July–August–September (JJAS) from 2001 to 2005 with a focus on two  
111 contrasting years, 2003 (above normal precipitation year) and 2004 (below normal  
112 precipitation year). The two years, 2003 and 2004 (respectively, the wettest and driest years  
113 among the five years), were selected to estimate the limits of the impact of internal soil  
114 moisture forcing on the new non-hydrostatic dynamical core of RegCM4. Several previous  
115 studies used two extreme years for their sensitivity study of initial soil moisture conditions on  
116 the models (e. g., Hong et al., 2000; Kim and Hong, 2006). We set up an ensemble of three  
117 experiments, each with simulations starting from June 1 to September 30. For each  
118 experiment, we applied (i) a reference initial soil moisture condition, (ii) a wet initial soil  
119 moisture condition, and (iii) a dry initial soil moisture condition. Kang et al. (2014) compared  
120 different land surface schemes (BATS and CLM3) and different spin-up periods to simulate  
121 June–July–August precipitation and recommended a 7-day spin-up period. In this study, we  
122 used CLM4.5 as the land surface scheme (Oleson et al., 2013), which has a more complex  
123 design. The first seven days (Kang et al., 2014) were excluded from the analysis as a spin-up  
124 period. We used the soil moisture from the reanalysis of the European Centre Meteorological  
125 Weather Forecast’s Reanalysis of the 20th century (ERA20C) to initialize the control runs.  
126 Wet and dry experiments were initialized for the soil moisture (in volumetric fraction  $m^3 \cdot m^{-3}$ )

127 3) at the maximum (= 0.489) and minimum (= 0.117.10<sup>-4</sup>) soil moisture values over West  
128 Africa derived from the ERA20C soil moisture dataset.

## 129 **2.2 Validation datasets and evaluation metrics**

130 Our investigation focused on the air temperature at 2 m and the precipitation over the West  
131 African domain during JJAS for 2003 and 2004. The simulated precipitation fields are  
132 validated with two observation datasets: the Climate Hazards Group Infrared Precipitation  
133 Stations (CHIRPS) dataset from the University of California at Santa Barbara, available from  
134 1981 to 2020 with 0.05° high-resolution data and the Tropical Rainfall Measuring Mission  
135 3B43V7 (TRMM) dataset with 0.25° high-resolution data available from 1998 to 2013  
136 (Huffman et al., 2007). We validated the 2-m temperature using two observation datasets: **the**  
137 **NOAA CPC global daily temperature from the Global Telecommunication System (GTS),**  
138 gridded at a horizontal resolution of 0.5° from 1979 to 2020 (Fan Y. and Huug van den Dool,  
139 2008), and daily temperature from ERA-Interim (EIN) reanalysis at 0.25° of horizontal  
140 resolution available from 1979 to 2020 (Dee et al., 2011). To compare the model simulations  
141 with the observation datasets, we re-gridded all the products to 0.22° × 0.22° using a bilinear  
142 interpolation method (Nikulin et al., 2012).

143 The performance of RegCM4-CLM4.5 to simulate the extreme indices was evaluated using  
144 four selected sub-regions (Fig. 1) based on the previous work of Koné et al. (2018), which  
145 correspond to different annual precipitation cycle features. We used the mean bias (MB),  
146 which captures the small-scale differences between the simulation and observation. The  
147 pattern correlation coefficient (PCC) is also used as a spatial correlation between model  
148 simulations and observations to indicate the large-scale similarity degree.

149 To quantify the impact of soil moisture anomalies on climate extremes, in their work over  
150 Asia, Liu et al. (2014) used the MBs in five subregions. In our study, we used the MBs and  
151 the probability density functions (PDF, Gao et al. (2016); Jaeger and Seneviratne (2011)) for  
152 this purpose to better capture how many grid points are impacted by initial soil moisture and  
153 their highest value.

154 **Significance of differences was tested for the control vs. sensitivity experiments. We used a**  
155 **two-tailed Student's t-test at each grid point as in Liu et al. (2014) over Asia.** Owing to the  
156 multiplicity problem of independent tests and the spatial dependency of neighboring! grid  
157 points, the significant results can only be seen as a crude estimate. Therefore, we perform the

158 land point area-weighted fraction with a statistical significance of 10% and display the  
159 seasonal extreme indices maps for 2003 and 2004.

160

### 161 **2.3. Extreme rainfall and temperature indices**

162 In this study, to investigate the changes in precipitation and temperature in terms of duration,  
163 occurrence, and intensity, six extreme temperature and four extreme rainfall indices were  
164 examined using daily minimum and maximum temperature and daily rainfall data (Table 1).  
165 These ten extreme indices are recommended by the Expert Team on Climate Change  
166 Detection and Indices (ETCCDI, Peterson et al., 2001). We estimated the monthly values of  
167 the indices, which allowed us to investigate seasonal variations.

## 168 **3. Results and discussion**

### 169 **3.1. Seasonal extreme rainfall**

170 In this section, we analyse six extreme rainfall indices based on daily precipitation in  
171 RegCM4 simulations over West Africa. All precipitation indices were calculated for JJAS in  
172 2003 and 2004. Table 2 summarizes the PCC and the MB of all precipitation indices studied  
173 in this section for TRMM observation and model simulations derived from control  
174 experiments with reanalysis of the initial soil moisture ERA20C with respect to CHIRPS  
175 observations, calculated for the west Sahel, central Sahel, Guinea coast, and the entire West  
176 African domain during JJAS 2003 and 2004.

177

#### 178 **3.1.1 The index of the number of the wet days (R1mm index)**

179 Figure 2 shows the mean values of the number of wet days (R1mm index, in days) from  
180 CHIRPS (Fig. 2a, d) and TRMM (Fig. 2b, e) observations and their corresponding simulated  
181 control experiments (Fig. 2c, f) with the initial soil moisture derived from ERA20C  
182 reanalysis. We have chosen CHIRPS because of its high resolution, mainly because this  
183 product has been widely assessed and used for the study of extreme events in West Africa by  
184 Bichet et al. (2018a, b) and Didi et al. (2020). The two observation datasets CHIRPS (Fig. 2a,  
185 d) and TRMM (Fig. 2b, e) show a similar large-scale pattern over the West African domain  
186 with a PCC up to 0.98 (Table 2). The maximum values of the R1mm index were located over  
187 mountainous regions such as the Cameroon Mountains, Jos Plateau, and Guinea Highlands,  
188 while the minimum values of the R1mm index were found over the Sahel with the number of  
189 wet days decreasing gradually from south to north. However, although the large-scale patterns

190 were similar, at the local scale, some differences were found in terms of the magnitude and  
191 spatial extent of these maxima and minima. The TRMM datasets underestimated the number  
192 of wet days over the central and west Sahel, and they were overestimated over the Guinea  
193 coast for both JJAS 2003 and JJAS 2004 (Table 2). A strongest underestimation was observed  
194 over the central Sahel with MB of approximately -6.76 and -7.51 days for JJAS 2003 and  
195 JJAS 2004, respectively (Table 2). However, the strongest overestimation was found over the  
196 Guinea coast with MB reached 8.89 and 10.44 days for JJAS 2003 and JJAS 2004,  
197 respectively (Table 2).

198 The control experiments (Fig. 2c, f) reproduced well the large-scale structure of the observed  
199 rainfall, with PCC values of 0.96 and 0.95 for JJAS 2003 and JJAS 2004, respectively (Table  
200 2) over the entire West African domain, but did exhibit some spatial extent and magnitude  
201 biases at the local scale. The control experiment displayed a large and quite homogeneous  
202 area of maximum values of the R1mm index below 12° N latitude. The control experiments  
203 overestimate the number of wet days over most of the studied domains (Table 2). The largest  
204 MBs were found over the Guinea coast with MB more than 53.16 and 55.46 days for JJAS  
205 2003 and JJAS 2004, respectively (Table 2). This overestimation of the number of wet days in  
206 RegCM4 was also found by Thanh et al. (2017) with RegCM4 for Asia.

207 Figure 2 (second panel) displays additional changes in the R1mm index for JJAS 2003 and  
208 JJAS 2004 for dry (Fig. 2g and i, for JJAS 2003 and JJAS 2004, respectively) and wet  
209 experiments (Fig. 2h and j, for JJAS 2003 and JJAS 2004, respectively) compared to their  
210 associated control experiments; the dotted area shows changes with statistical significance at  
211 the 10% level. The dry experiments (Fig. 2g, i) decrease the R1mm index while the wet  
212 experiments (Fig. 2h, j) favour an increase in the R1mm index, especially over central Sahel  
213 and a small part of west Sahel. The impact of initial soil moisture on R1mm was linear over  
214 central Sahel. However, over the Guinea coast sub-region, both wet and dry experiments  
215 showed a significant increase in R1mm.

216 For a better quantitative evaluation, Fig. 3 displayed the PDF distributions of the changes in  
217 the R1mm index over the studied domains (Fig. 1), during JJAS 2003 and 2004. Table 4  
218 summarizes the maximum values of changes obtained on the PDF's for extreme precipitation  
219 indices used in this study. The results essentially confirmed the linear impact found over  
220 central Sahel (Fig. 3a). Over west Sahel, the Guinea coast, and the West African domain (Fig.  
221 3b, c, and d), both dry and wet experiments led to an increase in the R1mm index. The

222 strongest R1mm index increase (decrease) was observed in wet (dry) experiments over west  
223 (central) Sahel, with a maximum change of approximately 12 days (-5.19 days) for JJAS 2003  
224 (Table 4).

225 Summarizing the results of this section, RegCM4 overestimates the number of wet days over  
226 most of the studied domains. A linear impact on the R1mm index for the dry (wet)  
227 experiments was found over the central Sahel, with a decrease (increase) in R1mm index.  
228 These results were compatible with previous work that sustained a strong land–atmosphere  
229 coupling in areas between wet and dry climate regimes (Zhang et al., 2011; Koster et al.,  
230 2006. The strongest R1mm index increase (decrease) was observed in wet (dry) experiments  
231 over west (central) Sahel, with a maximum change of approximately 12 days (-5.19 days) for  
232 JJAS 2003.

233

### 234 **3.1.2 Simple daily intensity index (SDII).**

235 We analyzed in this section the SDII index which gives the amount of precipitation mean on  
236 wet days (daily precipitation >1mm). Figure 4 (first panel) is the same as Fig.2 (first panel)  
237 but shows the amount of precipitation mean on wet days (SDII index, in mm.day<sup>-1</sup>). Over the  
238 entire West African domain, the two observations products CHIRPS (Fig.4a, d) and TRMM  
239 (Fig.4b, e) presented a similar large-scale pattern with a PCC about 0.86 for both JJAS 2003  
240 and JJAS 2004 (Table 2). However, the maxima SDII index values are quite different in term  
241 of spatial extension and magnitude. Over the coastline of the Gulf of Guinea, CHIRPS  
242 datasets (Fig.4a, d) depicted the highest values of SDII index, more than 25 mm.day<sup>-1</sup>. While  
243 the SDII index values, in TRMM datasets not exceed 12 mm.day<sup>-1</sup> over most part of this  
244 region. Over the central and west Sahel, TRMM datasets showed large sparse values of SDII  
245 index up to 20 mm.day<sup>-1</sup>, while CHIRPS datasets not exceed 12 mm.day<sup>-1</sup> for both JJAS 2003  
246 and JJAS 2004. The largest underestimations of TRMM dataset with respect to CHIRPS  
247 were found over the Guinea coast sub-region with MB more than -5.24 and -6.44 mm.day<sup>-1</sup>  
248 (for JJAS 2003 and JJAS 2004, respectively; Table 2). However, strongest overestimations  
249 were observed over central Sahel with MB reaching 3.67 and 2.07 mm.day<sup>-1</sup> (for JJAS 2003  
250 and JJAS 2004, respectively; Table 2).

251 The control experiments (Fig. 4 c, f) reproduced well the large-scale pattern of observation  
252 products with a PCC reaching 0.73 and 0.77 (in JJAS 2003 and JJAS 2004, respectively;  
253 Table 2) over the West African domain. However, at the local scale, some biases were  
254 observed. Over most of the studied domains, the magnitude of the SDII was underestimated,



255 not exceeding  $10 \text{ mm}\cdot\text{day}^{-1}$ , except over the Cameroon Mountains (Fig. 4c, f). Therefore,  
256 precipitation events were less extreme in the control experiments. The largest MBs were  
257 located over the Guinea coast with MBs more than  $-13.62$  and  $-14.65 \text{ mm}\cdot\text{day}^{-1}$  (for JJAS  
258 2003 and JJAS 2004, respectively; Table 2).

259 Figure 4 (second panel) is the same as Fig. 2 (second panel), but the display changes in the  
260 amount of mean precipitation on wet days. Unlike the R1mm index, a change in the SDII was  
261 not linear over most of studied domains. In general, a similar mixture of both increase and  
262 decrease is shown for dry and wet experiments over most of the studied domains (Fig. 4,  
263 second panel).

264 Figure 5 displays PDFs of changes in SDII, as in Fig. 3. The PDFs showed a maximum  
265 change value centered approximately on zero (Table 4), indicating that change in the amount  
266 of mean precipitation on wet days for wet and dry experiments is not significant.

267 In summary, RegCM4 underestimated the amount of mean precipitation on wet days over all  
268 the domain studies. It is worth noting that precipitation events simulated by RegCM4 with the  
269 current parameterization were less extreme, and the SDII did not exceed  $10 \text{ mm}\cdot\text{day}^{-1}$  over the  
270 entire West African domain. The impact of precipitation amount on wet days of the dry and  
271 wet experiments is not significant and is not sensitive to the contrast of year over the entire  
272 studied domain.

### 273 **3.1.3 Maximum number of consecutive dry days (CDD index).**

274 The duration of consecutive dry days (CDD index), which represents the maximum number of  
275 consecutive dry days with precipitation less than  $1 \text{ mm}\cdot\text{day}^{-1}$  was analyzed in this section.

276 Figure 6 (first panel) is the same as Fig. 2 (first panel) but shows the maximum number of  
277 CDD (in days). CHIRPS datasets located the largest CDD index values over the Sahara, more  
278 than 50 days (Fig. 6a, d). The lowest values were found over the Guinea coast, with CDD  
279 index values, less than 8 days. Over the West African domain, both the CHIRPS and TRMM  
280 datasets showed quite similar large-scale features over the entire West African domain with  
281 PCC more than 0.92. However, at the local scale, the observation datasets exhibited some  
282 disparities. In general, these disparities related only to the spatial extent, especially over the  
283 Sahel region. In JJAS 2003, the band of CDD index values was in the range of [10; 20] days  
284 and extended farther into the Sahel region for TRMM than CHIRPS. For JJAS in 2004,  
285 TRMM observations (Fig. 6b, e) presented a narrower band of minimum CDD index values  
286 over the Guinea coast around latitude  $10^\circ \text{ N}$  than CHIRPS, which extended over the Guinea  
287 coast. TRMM observations underestimated the CDD index over the entire West African

288 domain, with MB approximately  $-2.29$  and  $-1.75$  days (for JJAS 2003 and JJAS 2004,  
289 respectively; Table 2).

290 The control experiments (Fig. 6c, f) over the entire West African domain, reproduced well the  
291 large-scale pattern of the observed rainfall with a PCC more than 0.85 and 0.89 (for JJAS  
292 2003 and JJAS 2004, respectively; Table 1). However, in terms of magnitude, some  
293 differences were observed at the local scale. In general, the control experiments overestimated  
294 the CDD index over most studied domains, except over the Guinea coast (Table 2). A  
295 strongest overestimation CDD index was observed over west Sahel with MB reaching more  
296 than 14.49 and 17.51 days (for JJAS 2003 and JJAS 2004, respectively; Table 2). The current  
297 model parameterization increase the drought extreme over most of the studied domains,  
298 except over the Guinea coast (Table 2).

299 Figure 6 (second panel) is the same as Fig. 2 (second panel) but shows changes in the  
300 maximum lengths of consecutive dry spells (through the CDD index). The initial soil moisture  
301 impact on CDD index was linear over the central and west Sahel (Fig. 6, second panel), and  
302 the dry (wet) experiments increase (decrease) the maximum lengths of consecutive dry spells  
303 (CDD index). However, particularly over the Guinea coast, the dry and wet experiments led  
304 to a decrease in CDD index.

305 Figure 7 is the same as Fig. 3 but displays the PDF distribution of the changes in the CDD  
306 index. The impact on the CDD index was linear over the central and west Sahel. A strongest  
307 increase (decrease) in the CDD index was observed over the central (west) Sahel in dry (wet)  
308 experiments with maximum change value reaching 3.80 ( $-12.73$ ) days in JJAS 2004 (2003)  
309 (Table 4).

310 In summary, RegCM4 overestimates the maximum number of consecutive dry days over most  
311 studied domains, except over the Guinea coast. The linear impact on CDD index was  
312 observed over the central and west Sahel, however, over the Guinea coast, the dry and wet  
313 experiments led to a decrease in CDD index.

#### 314 **3.1.4 Maximum number of consecutive wet days (CWD index).**

315 The persistence of wet spells (CWD index) which represents the maximum number of  
316 consecutive wet days with precipitation  $\geq 1$  mm.day<sup>-1</sup> is investigated in this section. Figure 8  
317 (first panel) is the same as Fig.2 (first panel) but shows the CWD index. The observation  
318 products TRMM (Fig.8b, e) and CHIRPS (Fig.8a, d) depicted a similar large-scale pattern  
319 with the PCCs reached 0.90 and 0.87 (resp. for JJAS 2003 and JJAS 2004, Table 2). CHIRPS  
320 observation located the maximum of CWD index over the mountain regions such as

321 Cameroon Mountains, Jos plateau and Guinea highlands and it is more than 20 days. While  
322 the minimum values of CWD index were found over most of the area above the latitude 17°N  
323 and did not exceed 4 days (Fig.8a, d). In general, the differences between TRMM and  
324 CHIRPS observation concerned the maxima magnitude and its extent, which are more  
325 pronounced in TRMM than CHIRPS. Generally, TRMM overestimated the CWD index over  
326 most of the studied domains compared to CHIRPS, except over central Sahel (Table 2). The  
327 strongest overestimation was found over the Guinea coast region with MB more than 2.47 and  
328 2.38 days (resp. for JJAS 2003 and JJAS 2004, Table 2).

329 The control experiments well reproduced the large-scale pattern over the entire West African  
330 domain, with PCCs values approximately 0.81 and 0.87 (resp. for JJAS 2003 and JJAS 2004,  
331 Table 2). However, at the local scale the control experiments exhibit some biases in the  
332 minimum and maximum CWD index values in term of magnitude and spatial extent. Control  
333 experiments overestimated the CDD index over most of domains studied (Fig. 8 c, f). We  
334 noted that, this overestimation area coincides with the excessive values of R1mm index  
335 (Fig.2c, f). The strongest overestimation was found over the Guinea coast, reaching 59.21 and  
336 60.51 days (resp. for JJAS 2003 and JJAS 2004, Table 2).

337 Figure 8 (second panel) is the same as Fig.2 (second panel), but displays changes in CWD  
338 index. As for R1mm index, over the central Sahel, the impact was linear, the dry (wet)  
339 experiments decrease (increase) CWD index for both JJAS 2003 and JJAS 2004. This result  
340 confirms the strong soil moisture impact over the transition zones with a climate between dry  
341 and wet regimes (Zhang et al., 2011; Koster et al., 2006). However, over Guinea and the west  
342 Sahel, the changes were not linear, both dry and wet experiments lead to cause an increase, in  
343 JJAS 2003 and JJAS 2004 (Fig. 8B, c).

344 Figure 9, as in Fig.3, but shows the PDF distribution of changes in CWD index. The linear  
345 impacts were observed over the central Sahel for both JJAS 2003 and JJAS 2004, and over  
346 west Sahel only in JJAS 2004 (Table 4). The strongest increase (decrease) on CWD index was  
347 found over central Sahel with maximum change reaching 15.58 (-4.48) days in wet (dry)  
348 experiments in JJAS 2004.

349 Summarizing the results of this section, as in R1mm and CDD indices, the CWD index was  
350 linear over the central Sahel for both JJAS 2003 and JJAS 2004, and over the west Sahel in  
351 JJAS 2004, that is, the dry (wet) experiments decrease (increase) the CWD index. The model  
352 RegCM4 overestimates the duration of wet days over most of studied domains. This

353 overestimation is linked with an excessive number of wet days as documented by Diaconescu  
354 et al. (2014).

355

### 356 **3.1.5 Maximum one-day precipitation accumulation (RX1day index).**

357 The maximum one-day precipitation accumulation (RX1day index) during JJAS 2003 and  
358 JJAS 2004 is assessed in this section. Figure 10 (first panel) shows the spatial distribution of  
359 the RX1day index. The observation datasets TRMM (Fig. 10b, e) and CHIRPS (Fig. 10 a, d)  
360 present notable differences in terms of the spatial extent of the maximum values of the  
361 RX1day index, although their large-scale pattern was similar with PCC of more than 0.84 for  
362 both JJAS 2003 and JJAS 2004 (Table 2). Over the Guinea and Sahel regions, the spatial  
363 extent of RX1day index maximum values more than 80 mm was large in the TRMM datasets,  
364 while CHIRPS datasets showed it confined over the coastline of the Gulf of Guinea. TRMM  
365 observations overestimated the RX1day index over the most of studied domains. The largest  
366 RX1day index was found over the central Sahel, with MB reaching 35.78 and 31.66 (for JJAS  
367 2003 and JJAS 2004, respectively; Table 2).

368 The control experiments captured the spatial pattern with PCC values of 0.50 and 0.4 (JJAS  
369 2003 and JJAS 2004, respectively; Table 2). This low coefficient of PCC was also obtained  
370 by Thanh et al. (2017) over Asia with RegCM4 (correlation < 0.3). The model simulations  
371 failed to capture the magnitude and spatial extent of the RX1day index maxima values. The  
372 control experiments underestimated the RX1day index over most of studied domains. The  
373 RX1day index was underestimated throughout studied domains; this was also due to the  
374 excessive light precipitation, simulated by the current physical parameterization of RegCM4.  
375 The largest underestimation was located over the Guinea coast and the west Sahel. For  
376 instance, over the west Sahel, the MB was approximately  $-38.07$  and  $-36.67$  mm (JJAS 2003  
377 and JJAS 2004, respectively; Table 2).

378 Figure 10 (second panel) is similar to Fig. 2 (second panel), but displays changes in the  
379 RX1day index. For the SDII, the impact of initial soil moisture anomalies on the RX1day  
380 index was not linear, and a similar mixture of increase and decrease in RX1day index is  
381 shown for dry and wet experiments over most of the studied domains (Fig. 10, second panel).  
382 Figure 11 is similar to Fig. 3, but shows the PDF distribution of changes in the RX1day index.  
383 The impact on RX1day index increase for both dry and wet experiments and was found over  
384 most of studied domains (Fig.11). The strongest increase in RX1day index was observed over  
385 Guinea in wet experiments 26.14 and 14.93 for JJAS 2003 and JJAS 2004, respectively.

386 In summary, RegCM4 underestimates the maximum one-day precipitation accumulation over  
387 most of studied domains. The impact on RX1day index increase for both dry and wet  
388 experiments and was found over most of studied domains.

389

### 390 **3.1.6 Precipitation percent due to very heavy precipitation days (R95pTOT index)**

391 In this section, we investigated the precipitation percentage due to very heavy precipitation  
392 days during JJAS 2003 and JJAS 2004. Figure 12 (first panel) is the same as Fig. 2 (first  
393 panel), but shows the spatial distribution of the R95pTOT index. TRMM (Fig. 12b, e) and  
394 CHIRPS observations (Fig. 12a, d) presented a similar spatial pattern over the entire West  
395 African domain, with a PCC value of 0.91 for both JJAS 2003 and JJAS 2004 (Table 2).  
396 However, some biases in spatial extent were noticed for R95pTOT index maxima. TRMM  
397 observation extended the maximum R95pTOT index over the Guinea and Sahel regions (Fig.  
398 10, first panel), while CHIRPS confined them over the Guinea coast. Overall, TRMM showed  
399 a dominant overestimation compared to CHIRPS over the West African domain by  
400 approximately 16.54% and 18.54 % (JJAS 2003 and JJAS 2004, respectively; Table 2). The  
401 control experiments (Fig. 12c, f) capture the spatial pattern with PCC values of 0.59 and 0.55  
402 (JJAS 2003 and JJAS 2004, respectively; Table 2). As with SDII and RX1day indices, the  
403 control experiments underestimated the values of the R95pTOT index, while they  
404 overestimated the R1mm index. This was also due to the current physical parameterisation  
405 scheme of the RegCM4 model, which results in a positive bias for the number of wet days  
406 with a low precipitation threshold (e. g., 1 mm•day<sup>-1</sup>), and a negative bias for the indices of  
407 the number of wet days with a higher precipitation threshold (e.g., 10 mm•day<sup>-1</sup>, not shown  
408 here).

409 The control experiments underestimated the R95pTOT index over the different studied  
410 domains. The largest underestimation of the R95pTOT index was located over the Guinea  
411 coast with MB more than -43.22 and -46.61 % (for JJAS 2003 and JJAS 2004, respectively;  
412 Table 2).

413 Figure 12 (second panel) is similar to Fig. 2 (second panel), but displays changes in the  
414 R95pTOT index. Both dry and wet experiments tended to cause an increase in the R95pTOT  
415 index over the orographic regions. Therefore, the initial soil moisture conditions, whether dry  
416 or wet, tended to reinforce extreme floods.

417 Figure 13 is the same as Fig. 3 but shows the PDF distribution of changes in the R95pTOT  
418 index indicating an increase in the R95pTOT index for both wet and dry experiments over

419 most of the studied domains. The strongest increase in R95pTOT index was found over the  
420 west Sahel and Guinea coast with maximum change values around 4.03% (JJAS 2004) and  
421 4.33% (JJAS 2003), respectively (Table 4).

422 In summary, RegCM4 underestimates the precipitation percentage due to very heavy  
423 precipitation days over the West African domain. The initial soil moisture conditions, whether  
424 dry or wet, accentuate the precipitation percent due to very heavy precipitation days. This  
425 result is consistent with Liu et al.'s (2014) work over Asia using RegCM4. The impact on  
426 R95pTOT index led to an increase in wet and dry experiments over most of the studied  
427 domains.

428

### 429 **3.2. Seasonal temperature extreme indices**

430 In this section, using daily maximum and minimum temperatures, we analyze four extreme  
431 temperature indices (Table 1) in RegCM4 simulations over West Africa. All temperature  
432 indices were calculated for JJAS 2003 and JJAS 2004. Table 3 summarizes the PCC and MB  
433 of all temperature indices studied in this section for EIN reanalysis and model simulations  
434 derived from control experiments with initial soil moisture from ERA20C reanalysis, with  
435 respect to GTS observations, calculated over the domains presented in Fig. 1, during the JJAS  
436 2003 and JJAS 2004.

437

#### 438 **3.2.1. Maximum value of daily maximum temperature (TXx index)**

439 In this section, we analyze the TXx index, which gives the hottest day's temperature during  
440 JJAS 2003 and JJAS 2004. Figure 14 (first panel) shows the TXx index (in °C) from GTS  
441 observations (Fig. 14a, d) and EIN reanalysis (Fig. 14b, e) for JJAS 2003 and JJAS 2004 and  
442 their corresponding simulated control experiments (Fig. 14c, f) with the initial soil moisture  
443 of the reanalysis ERA20C. The GTS observation showed the highest values of the TXx index  
444 observed over the Sahara, at more than 46 °C. The lowest values (less than 32 °C) were found  
445 over the Guinea coast (Fig. 14a, d). Fan Y. and Huug van den Dool (2008) in their work  
446 showed that the Reanalysis 2 m temperature data sets may not be suitable for model forcing  
447 and validation. We have chosen NOAA-CPC GTS observation dataset as reference in this  
448 study over ERA-Interim reanalysis, because NOAA-CPC GTS consists of a blending of  
449 satellite-based data collection and in situ data archive available in the GTS (Global  
450 Telecommunication System). The EIN reanalysis has similar large-scale patterns with a PCC

451 value of 0.99 over the entire West African domain (Table 3). However, some local biases are  
452 shown for magnitude and spatial extent of these maxima and minima. The reanalysis of the  
453 EIN (Fig. 14b, e) shows lower values (less than 28 °C) of the TXx index over a large area  
454 along the Guinea coastline compared to GTS datasets. Conversely, GTS observation  
455 presented higher values of the TXx index (up to 48 °C) over a large area compared to the EIN  
456 reanalysis (Fig.14a, d), which showed a negative bias of the TXx index over most of the  
457 studied domains (Table 3).

458 The control experiments (Fig. 14c, f) reasonably replicate the large-scale patterns of the TXx  
459 index values with PCCs up to 0.99 ( Table3) over the entire West African domain; however,  
460 they exhibited some biases at a local scale. The control experiments were closer to the  
461 maximum and minimum values displayed in the GTS observation. The control simulations  
462 overestimated the TXx values over the central and west Sahel, and over the Guinea coast  
463 (Table 3). The greatest overestimation was found over the west Sahel with MB of  
464 approximately 3.02 and 2.02 °C (for JJAS 2003 and JJAS 2004, respectively; Table 3).  
465 However, the biases obtained for the TXx index in this study were much lower than those  
466 obtained by Thanh et al. (2017), who used RegCM4 over Asia where it reached 8 °C.

467 Figure 14 (second panel) displays changes in the TXx index for JJAS 2003 and JJAS 2004 for  
468 dry (Fig. 14g, i for JJAS 2003 and JJAS 2004, respectively) and wet experiments (Fig. 14h, j  
469 for JJAS 2003 and JJAS 2004, respectively) with respect to their corresponding control  
470 experiments; the dotted area shows changes with a statistical significance of 10%. The impact  
471 of the initial soil moisture conditions on the TXx index was linear over most of studied  
472 domains; that is, the dry experiments led to an increase in the TXx index values, while the wet  
473 experiments favoured a decrease in the TXx index values.

474 The PDF distributions of TXx index changes for JJAS 2003 and JJAS 2004 over (a) the  
475 central Sahel, (b) West Sahel, (c) Guinea, and (d) West Africa derived from dry and wet  
476 experiments compared to the corresponding control experiments are shown in Fig. 15. Table 5  
477 summarizes the maximum values of changes obtained on the PDF's for extreme temperature  
478 indices used in this study. As mentioned above, the results confirmed the linear impact on the  
479 TXx index over most of studied domains (Fig. 15). The strongest decrease (increase) in the  
480 TXx index was found over the central Sahel with a maximum change values around  $-2.57$  °C  
481 (more than 1.69 °C) in wet (dry) experiments in JJAS 2004.

482 In summarizing this section, during JJAS 2003 and 2004, the RegCM4 model overestimates  
483 and underestimates the hottest day's temperature over the Sahel (west and central) and Guinea  
484 coast. The impact on the TXx index is linear over most of studied domains; that is, the dry  
485 (wet) experiments decrease (increase) the TXx index.

486

### 487 **3.2.2. Minimum value of daily maximum temperature (TXn index).**

488 In this section, we investigated the TXn index which gives the lowest day's temperature  
489 during JJAS 2003 and JJAS 2004. Figure 16 (first panel) is the same as Fig.14 (first panel)  
490 but presents the spatial distribution of the TXn index. GTS observation (Fig.16a, d) and EIN  
491 reanalysis (Fig.16b, e) display similar features with PCC reached 0.99 (for JJAS 2003 and  
492 JJAS 2004, Table 3). The maxima and minima values of TXn index were located over the  
493 Sahara and the Guinea coast respectively. However, there were some differences at the local  
494 scale in terms of spatial extent and magnitude. The EIN reanalysis presented a larger spatial  
495 extent of the maxima (greater than 36°C) and minima (less than 24°C) compared to GTS  
496 observation. Generally, the EIN reanalysis showed a negative bias value over most of the  
497 studied domains (for both JJAS 2003 and JJAS 2004 Table3. The strongest negative bias was  
498 found over the west Sahel with MB of approximately -1.48 and -1.73°C (resp. for JJAS 2003  
499 and JJAS 2004, Table 3).

500 The control experiments showed a good agreement with the GTS datasets in the large scale  
501 patterns with PCC of approximately 0.99, however, the magnitude of the TXn index over  
502 most of studied domains was overestimated. The strongest positive bias was observed over  
503 west Sahel domain, the MB of approximately 6.56 and 5.44 °C (resp. JJAS 2003 and JJAS  
504 2004, Table 3). The biases obtained in this study were lower than those of a similar study  
505 carried out by Thanh et al. (2017) over Asia using RegCM4.

506 As for Fig.14 (second panel), the Figure 16 (second panel) displayed changes in TXn index.  
507 The impact on TXn index of the initial soil moisture anomalies was linear over most of  
508 studied domains, that is, the dry experiments led to an increase of TXn index values while the  
509 wet experiments favor a decrease of TXn index values.

510 Figure 16 (second panel) is similar to Fig.14 (second panel) but displays the PDF distribution  
511 of changes in TXn index. The impact on TXn index was linear over most of the domain  
512 studied, although this impact is rather weak as compared to the TXx index. The strongest  
513 increase (decrease) in TXn index are found over the central (west) Sahel reaching 1.03 °C (-  
514 1.67°C) in dry (wet) experiments, in JJAS 2004 (JJAS 2004) (Table5).



515 In summary, RegCM4 overestimated the lowest day's temperature during JJAS 2003 and  
516 JJAS 2004 over the whole West African domain. As for TXx index, the impact on TXn index  
517 to soil moisture anomalies was linear over most of studied domains, that is, dry (wet)  
518 experiments cause an increase (decrease) of TXn index values.

519

### 520 **3.2.3. Minimum value of daily minimum temperature (TNn index).**

521 In this section, we examine the TNn index, which gives the lowest temperature at night during  
522 JJAS 2003 and JJAS 2004. Figure 18 (first panel) is the same as Fig. 14 (first panel) but  
523 displays the spatial distribution of the TNn index. GTS observations (Fig. 18 a, d) show the  
524 maxima of TNn index values above 15° N latitude, not exceeding 27 °C, while the minima  
525 values are less than 17 °C and are located over the mountainous regions such as the Cameroon  
526 Mountains, Jos Plateau, and Guinea Highlands. The EIN reanalysis showed a similar spatial  
527 pattern as GTS observation, with a PCC value of approximately 0.99 over the entire West  
528 African domain (Table 3) despite some biases at the local scale. The EIN reanalysis (Fig. 18  
529 b, e) displayed the highest value of the TNn index (exceeding 27 °C) compared to GTS  
530 observation, and were located over a large area above 15° N. The EIN reanalysis also showed  
531 the lowest values (less than 21 °C) of the TNn index compared to the GTS observation,  
532 located over the orographic regions. The EIN reanalysis overestimated the TNn index values  
533 over most of the studied domains. The strongest positive bias was observed over the west  
534 Sahel, the MB reached 3.43 and 2.98 °C for JJAS 2003 and JJAS 2004, respectively (Table  
535 3).

536 The control experiments (Fig. 18 c, f) showed good agreement with GTS observations with  
537 PCC values of approximately 0.99; however, they exhibited some biases at the local scale.  
538 The control experiments overestimated the magnitude of the TNn index over most of studied  
539 domains.

540 The strongest positive bias was observed over the west Sahel, the MB was approximately 3.30  
541 °C and 2.55 °C for JJAS 2003 and JJAS 2004, respectively (Table 3). These positive biases  
542 obtained in simulating the TXx, TXn, and TNn indices were opposite to the cold bias known  
543 from RegCM4 in mean climate simulation (Koné et al., 2018, Klutse et al., 2016). It is  
544 difficult to determine the origin of RegCM4 temperature biases, as they can depend on several  
545 factors, such as surface energy fluxes and water, cloudiness, and surface albedo (Sylla et al.,  
546 2012; Tadross et al., 2006).

547 Figure 18 (second panel) is the same as Fig. 14 (second panel), but displays changes in the  
548 TNn index. Over the central and west Sahel, both dry and wet experiments led to a decrease.  
549 Conversely, over the Guinea coast, we found an increase.

550 Figure 19 is the same as Fig. 15 but shows the PDF distribution of changes in the TNn index.  
551 A linear impact was found over west Sahel and Guinea coast only in JJAS 2004, that is, wet  
552 (dry) experiments increase (decrease) the TNN index (Fig.19; Table 5). The strongest increase  
553 (decrease) in TNn index in wet (dry) experiment was found over Guinea coast (west Sahel),  
554 with maximum change values around 0.11 °C and (−1.15 °C) in JJAS 2004 (JJAS 2003)  
555 (Table 5).

556 In summary, RegCM4 overestimated the lowest temperature at night during JJAS 2003 and  
557 JJAS 2004 over the different studied domains. A linear impact was found over west Sahel and  
558 Guinea coast only in JJAS 2004, that is, wet (dry) experiments increase (decrease) the TNN  
559 index

#### 560 **3.2.4. Maximum value of daily minimum temperature (TNx index)**

561 In this section, we turned our attention to TNx index, which gives the warmest night  
562 temperature during JJAS 2003 and JJAS 2004. Figure 20 (first panel) is the same as Fig. 14  
563 (first panel), but for the TNx index. GTS observations (Fig. 20 a, d) showed that the maxima  
564 of the TNx index values over the Sahara reached 40 °C, while the minima around 24 °C were  
565 located over the Guinea coast sub-region. The EIN reanalysis (Fig. 20b, e) showed similar  
566 large-scale patterns with PCC values of 0.99, but some biases can be noticed between the  
567 GTS and EIN datasets. The EIN reanalysis underestimated the maxima (not exceeding 38 °C)  
568 and minima (less than 22 °C) located over the Sahara and the orographic regions such as the  
569 Cameroon Mountains, Jos Plateau, and Guinea Highlands. The EIN reanalysis displayed  
570 negative MB over the Guinea coast with MB approximately −3.11 °C and −3.14 °C (JJAS  
571 2003 and JJAS 2004, respectively; Table 3).

572 The control experiments (Fig. 20c, f) successfully reproduced the general features of the TNx  
573 index with a PCC value of 0.99, but some differences were shown at the local scale. Unlike  
574 the TNn index, the control experiments underestimated the TNx index over most of the  
575 studied domains. The strongest negative bias was found over the central Sahel, MB was  
576 approximately −3.35 °C and −3.32 °C (for JJAS 2003 and JJAS 2004, respectively; Table 3).  
577 This underestimation of the TNx index seems to be systematically related to the cold bias in  
578 RegCM4 over West Africa, which has been reported in several papers (Koné et al., 2018,  
579 Klutse et al., 2016).

580 Figure 20 (second panel) is the same as Fig. 14 (second panel) but displays changes in the  
581 TNx index. Like for the TNn index, the impact on the TNx index of initial soil moisture  
582 conditions was somewhat linear over the central Sahel, and dry experiments led to an increase  
583 in the TNx index values, while the wet experiments favoured a decrease in the TNx index  
584 values. However, over the west Sahel, both wet and dry experiments led to a dominant  
585 decrease. Conversely, over the Guinea coast, although the signal was weak, both dry and wet  
586 experiments led to a dominant increase.

587 Figure 21 is the same as Fig. 15 but displays the PDF distributions of the changes in the TNx  
588 index. Like for the TNn index, the impact on the TNx index changes was linear over the  
589 central Sahel. The strongest increase (decrease) in TNx index was found over the central  
590 Sahel in dry (wet) experiments with maximum change approximately 0.25 ( $-1.67$  °C) in JJAS  
591 2003 (JJAS 2004) (Table 5).

592 In summary, RegCM4 underestimates the warmest night temperature during JJAS 2003 and  
593 JJAS 2004 over most of studied domains. The impact on the TNx index of initial soil  
594 moisture conditions was linear over the central Sahel, that is, dry (wet) experiments led to an  
595 increase (decrease) in the TNx index values.

596

#### 597 **4. Conclusions**

598 The impact on the subsequent summer extreme climate of the initial soil moisture conditions  
599 over West Africa was investigated using the RegCM4-CLM45. In addition, the performance  
600 of RegCM4-CLM4.5 in representing six extreme indices of precipitation and four extreme  
601 indices of temperature over West Africa was also evaluated. Results have been presented for  
602 JJAS 2003 (wet year) and JJAS 2004 (dry year). We performed sensitivity studies over the  
603 West African domain, with a spatial resolution of 25 km. We initialized the control runs using  
604 ERA20C reanalysis soil moisture, at its maximum and minimum values over the West Africa  
605 domain, respectively, for dry and wet experiments.

606 Compared to the extreme indices of the observation datasets, the model overestimated and  
607 underestimated the number of wet days for a low ( $1 \text{ mm}\cdot\text{day}^{-1}$ ) and high threshold rain rate  
608 (e.g.,  $10 \text{ mm}\cdot\text{day}^{-1}$ , not shown here). RegCM4 also underestimated the simple precipitation  
609 intensity index (SDII), the maximum 1-day precipitation (Rx1day index), and the  
610 precipitation percentage due to very heavy precipitation days (R95pTOT index). The current  
611 physical parameterization scheme of the RegCM4 model used in our study results in a

612 positive bias for the number of wet days with a low precipitation threshold (e. g. 1 mm•day-  
613 1), while in a negative bias for a higher precipitation threshold (e.g. 10 mm•day-1, not shown  
614 here). However, RegCM4 generally overestimated the maximum number of CWD and CDD  
615 over the West African domain studied. The temperature extreme indices used in this study  
616 (TXx, TXn, and TNn) were also overestimated, except the TNx index, which was  
617 underestimated over most of studied domains.

618 The impact on extreme precipitation indices of the initial soil moisture conditions was linear  
619 only for indices related over the central Sahel to the number of precipitation events (R1mm,  
620 CDD, and CWD indices) and not for those related to the amount of precipitation (SDII,  
621 RX1day, and R95pTOT). The dry and wet experiments accentuated the precipitation  
622 percentage due to very heavy precipitation days and maximum one-day precipitation  
623 accumulation (R95pTOT and RX1day indices, respectively) over most of the studied  
624 domains.

625 The initial soil moisture conditions unequally affected the daily maximum and minimum  
626 temperatures over the West African domain. There was a greater impact on daily maximum  
627 temperature extremes than on the daily minimum temperature extremes. These results are  
628 consistent with those of previous studies (Jaeger and Seneviratne, 2011; Zhang et al., 2009).

629 The wet (dry) experiments resulted in an increase (decrease) in the TXx and TXn indices over  
630 most of the studied. The impact of initial soil moisture conditions on the indices related to the  
631 minimum temperature (TNx and TNn indices) was linear only for TNx index over central  
632 Sahel. The dry (wet) experiments cause an increase (a decrease) in the TNx.

633 This study helps to understand the impact of the initial soil moisture conditions on extreme  
634 events of precipitation and temperature in terms of intensity, frequency and duration over  
635 West Africa. This is a contribution to the improvement of extreme event forecasts in West  
636 Africa in highlighting the crucial role of initial soil moisture. For a proper assessment of the  
637 dependence of the model in our results, it would be appropriate to repeat the investigation  
638 using different RCMs in a multi-model framework.

639

640

641 **Author contribution**

642 The authors declare to have no conflict of interest with this work. B. Koné and A. Diedhiou  
643 fixed the analysis framework. B. Koné carried out all the simulations and figures production  
644 according to the outline proposed by A. Diedhiou. B. Koné and A. Diedhiou, S. Anquetin and  
645 A. Diawara worked on the analyses. All authors contributed to the drafting of this manuscript.

646

647 **Acknowledgements**

648 The research leading to this publication is co-funded by the NERC/DFID “Future Climate for  
649 Africa” programme under the AMMA-2050 project, grant number NE/M019969/1 and by  
650 IRD (Institut de Recherche pour le Développement; France) grant number UMR IGE  
651 Imputation 252RA5.

652

653 **References:**

654

655 Bichet, A., & Diedhiou, A. (2018a). West African Sahel has become wetter during the last 30  
656 years, but dry spells are shorter and more frequent. *Climate Research*, 75(2), 155-162.

657

658 Bichet, A., & Diedhiou, A. (2018b). Less frequent and more intense rainfall along the coast of  
659 the Gulf of Guinea in West and Central Africa (1981–2014). *Climate Research*, 76(3), 191-  
660 201.

661

662 Danielson J.J., and Gesch D.B.: Global multi-resolution terrain elevation data 2010  
663 (GMTED2010): U.S. Geological Survey Open-File Report 2011–1073, 26 p, 2011.

664

665 Didi Sacré Regis M , Mouhamed, L., Kouakou, K., Adeline, B., Arona, D., Koffi Claude A,  
666 K., ... & Issiaka, S. (2020). Using the CHIRPS Dataset to Investigate Historical Changes in  
667 Precipitation Extremes in West Africa. *Climate*, 8(7), 84.

668

669 Dee D. P., Uppala S. M., Simmons A. J., Berrisford P., Poli P., Kobayashi S., Andrae U.,  
670 Balmaseda, M. A., Balsamo G., Bauer, P., Bechtold P., Beljaars A. C. M., van de Berg L.,  
671 Bidlot J., Bormann N., Delsol C., Dragani R., Fuentes M., Geer A. J., Haimberger L., Healy

672 S. B., Hersbach H., Hólm E. V., Isaksen L., Kállberg P., Köhler M., Matricardi M., McNally  
673 A. P., Monge-Sanz B. M., Morcrette J.-J., Park, B.-K., Peubey C., de Rosnay P., Tavolat C.,  
674 Thépaut J.-N. and Vitart F.: The ERA-Interim reanalysis: configuration and performance of  
675 the data assimilation system, *Q. J. Roy. Meteorol. Soc.*, 137, 553-597,  
676 <https://doi.org/10.1002/qj.828>, 2011.

677

678 Diaconescu E. P., Gachon P. , Scinocca J., and LapriseR.: Evaluation of daily precipitation  
679 statistics and monsoon onset/retreat over west Sahel in multiple data sets. *Climate Dyn.*, 45,  
680 1325–1354, doi:10.1007/s00382-014-2383-2, 2015 .

681

682 Easterling, D.R., Meehl, G.A., Parmesan, C., Changnon, S.A., Karl, T.R. and Mearns, L.O.:  
683 Climate Extremes: Observations, Modeling and Impacts. *Science* , 289, 2068-2074.  
684 <https://doi.org/10.1126/science.289.5487.2068>, 2000.

685

686 Emanuel K. A.: A scheme for representing cumulus convection in large-scale models. *Journal*  
687 *of the Atmospheric Science* 48: 2313–2335, 1991.

688

689 Fan Y., and van den Dool H. : A global monthly land surface air temperature analysis for  
690 1948 -present, *J. Geophys. Res.* 113, D01103, doi: 10.1029/2007JD008470, 2008.

691

692 Folland C. K., Palmer T. N. , and Parker D. E.: Sahel rainfall and worldwide sea  
693 temperatures, *Nature*, 320, 602 – 607, 1986.

694

695 Fontaine B., Janicot S. , and Moron V. : Rainfall anomaly patterns and wind field signals over  
696 West Africa in August (1958 – 1989), *J. Clim.*, 8, 1503 –1510, 1995.

697

698 Giorgi F., Coppola E., Solmon F., Mariotti L., Sylla M. B., Bi X., Elguindi N., Diro G. T.,  
699 Nair V., Giuliani G., Cozzini S., Guettler I., O'Brien T., Tawfik A., Shalaby A., Zakey A. S.,  
700 Steiner A., Stordal F., Sloan L., and Brankovic C. : RegCM4: model description and  
701 preliminary tests over multiple CORDEX domains, *Clim. Res.*, 52, 7–29,  
702 [doi.org/10.3354/cr01018](https://doi.org/10.3354/cr01018), 2012.

703

704 Grell G., Dudhia J. and Stauffer D. R.: A description of the fifth generation Penn State/NCAR  
705 Mesoscale Model (MM5), National Center for Atmospheric Research Tech Note NCAR/TN-  
706 398+STR, NCAR, Boulder, CO, 1994.  
707

708 Holtslag A., De Bruijn E., and Pan H. L. : A high resolution air mass transformation model  
709 for short-range weather forecasting, *Mon. Weather Rev.*, 118, 1561–1575, 1990.  
710

711 Hong S. Y. and Pan H. L.: Impact of soil moisture anomalies on seasonal, summertime  
712 circulation over North America in a regional climate model. *J. Geophys. Res.*, 105 (D24), 29  
713 625–29 634, 2000.  
714

715 Huffman, G. J., Adler, R. F., Bolvin, D. T., Gu, G., Nelkin, E. J., Bowman, K. P., Hong, Y,  
716 Stocker, E. F., and Wolff, D. B.: The TRMM multisatellite precipitation analysis: quasi-  
717 global, multiyear, combined-sensor precipitation estimates at fine scale, *J. Hydrometeorol.*, 8,  
718 38–55, 2007.  
719

720 Jaeger E. B., and Seneviratne S. I. : Impact of soil moisture-atmosphere coupling on  
721 European climate extremes and trends in a regional climate model, *Clim. Dyn.*, 36(9-10),  
722 1919-1939, doi:10.1007/s00382-010-0780-8, 2011.  
723

724 Kang S, Im E.-S. and Ahn J.-B.: The impact of two land-surface schemes on the  
725 characteristics of summer precipitation over East Asia from the RegCM4 simulations *Int. J.*  
726 *Climatol.* 34: 3986–3997, 2014.  
727

728 Kim J-E., and Hong S-Y.: Impact of Soil Moisture Anomalies on Summer Rainfall over East  
729 Asia: A Regional Climate Model Study, *Journal of Climate*. Vol. 20, 5732–5743, DOI:  
730 10.1175/2006JCLI1358.1, 2006.  
731

732 Kiehl J. T., Hack J. J., Bonan G. B., Boville, B. A., Briegleb B. P., Williamson D. L., and  
733 Rasch P. J.: Description of the NCAR Community Climate Model (CCM3), Technical Note  
734 NCAR/TN–420+STR, 152, 1996.  
735

736 Koné B., Diedhiou A., N'datchoh E. T., Sylla M. B. , Giorgi F., Anquetin S., Bamba A.,  
737 Diawara A., and Koba A. T.: Sensitivity study of the regional climate model RegCM4 to  
738 different convective schemes over West Africa. *Earth Syst. Dynam.*, 9, 1261–1278.  
739 <https://doi.org/10.5194/esd-9-1261-2018>, 2018.

740  
741

742 Koster R. D., GUO Z. H., Dirmeyer P. A., Bonan G., Chan E., Cox P., Davies H., Gordon C.  
743 T., Gordon C. T., Lawrence D., Liu P., Lu C. H, Malyshev S., McAvaney B., Mitchell K,  
744 Mocko D., Oki K., Oleson K., Pitman A., Sud Y. C. , Taylor C. M., 16 Versegny D., Vasic  
745 R., Xue Y., Yamada T.: The global land–atmosphere coupling experiment. Part I: Overview,  
746 *J. Hydrometeorol.*, 7(4), 590–610, doi:10.1175/JHM510.1, 2006.

747

748 Larsen J.: Record heat wave in Europe takes 35,000 lives. Earth Policy Institute, 2003.

749

750 Le Barbé L., Lebel L., and Tapsoba D.: Rainfall variability in west africa during the years  
751 1950-1990. *J. Climate*, 15 :187–202., 2002.

752

753 Loveland TR, Reed BC, Brown JF, Ohlen DO, Zhu Z, Yang L, J. W. Merchant J. W.:  
754 Development of a global land cover characteristics database and IGBP DISCover from 1km  
755 AVHRR data. *International Journal of Remote Sensing* 21: 1303–1330, 2000.

756

757 Liu D., G. Wang R. Mei Z. Yu, and Yu M. : Impact of initial soil moisture anomalies on  
758 climate mean and extremes over Asia, *J. Geophys. Res. Atmos.*, 119, 529–545,  
759 doi:10.1002/2013JD020890, 2014.

760

761 Klutse B. A. N., Sylla B. M., Diallo I., Sarr A., Dosio A., Diedhiou A., Kamga A., Lamptey  
762 B., Ali A., Gbobaniyi E. O., Owusu K., Lennard C., Hewitson B., Nikulin G., & Panitz H.-J.,  
763 Büchner M.: Daily characteristics of West African summer monsoon precipitation in  
764 CORDEX simulations. *Theor Appl Climatol.* 123:369–386 DOI 10.1007/s00704-014-1352-3,  
765 2016.

766



767 Nicholson, SE.: The nature of rainfall fluctuations in subtropical West-Africa. *Mon. Wea.*  
768 *Rev.* 22109, 2191-2208, 1980.

769

770 Nicholson SE.: Land Surface processes and Sahel climate. *Reviews of Geophysics.* 38(1),  
771 117-24139, 2000.

772

773 Nikulin G., Jones C., Samuelsson P., Giorgi F., Asrar G., Büchner M., Cerezo-Mota R.,  
774 Christensen O. B., Déque M., Fernandez J., Hansler A., van Meijgaard E., Sylla M. B. and  
775 Sushama L.: Precipitation climatology in an ensemble of CORDEX-Africa regional climate  
776 simulations, *J. Climate*, 6057–6078, <https://doi.org/10.1175/JCLI-D-11-00375.1>, 2012.

777

778 Oleson K., Lawrence D. M., Bonan G. B., Drewniak B., Huang M., Koven C. D., Yang Z.-L.:  
779 Technical description of version 4.5 of the Community Land Model (CLM) (No. NCAR/TN-  
780 503+STR). doi:10.5065/D6RR1W7M, 2013.

781

782 Pal J. S., Small E. E. and Elthair E. A.: Simulation of regional scale water and energy  
783 budgets: representation of subgrid cloud and precipitation processes within RegCM, *J.*  
784 *Geophys. Res.*, 105, 29579–29594, 2000.

785

786 Peterson T. C., Folland C., Gruza G., Hogg W. Mokssit A., Plummer N. : Report on the  
787 activities of the working group on climate change detection and related rapporteurs 1998-  
788 2001. Geneva (Switzerland): WMO Rep. WCDMP 47, WMO-TD 1071, 2001.

789

790 Philippon N., Mougín E. , Jarlan L. , and Frison P.-L.: Analysis of the linkages between  
791 rainfall and land surface conditions in the West African monsoon through CMAP, ERS-  
792 WSC, and NOAA-AVHR R data. *J. Geophys. Res.*, 110, D24115,  
793 doi:10.1029/2005JD006394, 2005.

794

795 Reynolds, R. W. and Smith, T. M.: Improved global sea surface temperature analysis using  
796 optimum interpolation, *J. Climate*, 7, 929–948, 1994.

797

798 Simmons A. S., Uppala D. D. and Kobayashi S.: ERA-interim: new ECMWF reanalysis  
799 products from 1989 onwards, *ECMWF Newsl.*, 110, 29–35, 2007.

800 Solmon F., Giorgi F., and Lioussé C.: Aerosol modeling for regional climate studies:  
801 application to anthropogenic particles and evaluation over a European/African domain, *Tellus*  
802 *B*, 58, 51–72, 2006.

803

804 Sundqvist H. E., Berge E., and Kristjansson J. E.: The effects of domain choice on summer  
805 precipitation simulation and sensitivity in a regional climate model, *J. Climate*, 11, 2698–  
806 2712, 1989.

807

808 Sylla MB, Giorgi F, Stordal F.: Large-scale origins of rainfall and temperature bias in high  
809 resolution simulations over Southern Africa. *Climate Res.* 52: 193–211, DOI:  
810 10.3354/cr01044, 2012.

811

812 Tadross MA, Gutowski WJ Jr, Hewitson BC, Jack C, New M.: MM5 simulations of  
813 interannual change and the diurnal cycle of southern African regional climate. *Theor. Appl.*  
814 *Climatol.* 86(1–4):63–80, 2006.

815

816 Thanh N.-D., Fredolin T. T., Jerasorn S., Faye C., Long T.-T., Thanh N.-X., Tan P.-V., Liew  
817 J., Gemma N., Patama S., Dodo G. and Edwin A.: Performance evaluation of RegCM4 in  
818 simulating extreme rainfall and temperature indices over the CORDEX-Southeast Asia  
819 region. *Int. J. Climatol.* 37: 1634–1647. Published online 28 June 2016 in Wiley Online  
820 Library ([wileyonlinelibrary.com](http://wileyonlinelibrary.com)) DOI: 10.1002/joc.4803, 2017.

821

822 Uppala S., Dee D., Kobayashi S., Berrisford P. and Simmons A.: Towards a climate data  
823 assimilation system: status update of ERA-interim, *ECMWF Newsl.*, 15, 12–18, 2008.

824

825 Wang, G., Yu, M., Pal, J. S., Mei, R., Bonan, G. B., Levis, S., and Thornton, P. E.: On the  
826 development of a coupled regional climate vegetation model RCM-CLM-CN-DV and its  
827 validation its tropical Africa, *Clim. Dynam.*, 46, 515–539, 2016.

828

829 You Q., Kang S., Aguilar E., Pepin N., Flügel W.-A., Yan Y. , Xu Y., Zhang Y. , and Huang  
830 J. : Changes in daily climate extremes in China and their connection to the large scale  
831 atmospheric circulation during 1961–2003, *Clim. Dyn.*, 36(11-12), 2399–2417,  
832 doi:10.1007/s00382-009-0735-0, 2010.

833

834 Zakey A. S., Solmon F., and Giorgi F.: Implementation and testing of a desert dust module in  
835 a regional climate model, *Atmos. Chem. Phys.*, 6, 4687–4704, [https://doi.org/10.5194/acp-6-](https://doi.org/10.5194/acp-6-4687-2006)  
836 4687-2006, 2006.

837

838 Zeng X., Zhao M. and Dickinson R .E.: Intercomparison of bulk aerodynamic algorithms for  
839 the computation of sea surface fluxes using TOGA COARE and TAO DATA, *J. Climate*, 11,  
840 2628-2644, 1998.

841

842 Zhang J, Wang W.C., and Wu L.: Land–atmosphere coupling and diurnal temperature range  
843 over the contiguous United States. *Geophys Res Lett* 36:L06706.  
844 doi:10.1029/2009GL037505, 2009.

845

846 Zhang J. Y., Wu L. Y. and Dong W. : Land-atmosphere coupling and summer climate  
847 variability over East Asia, *J. Geophys. Res.*, 116,D05117, doi 10.1029/2010JD014714, 2011.

848

849

850

851

852

853

854

855

856

857

858

859

860 **TABLES AND FIGURES.**

861

Extreme indices		Definition	Units
Extreme Rainfall Indices			
1	R1mm	Number of wet days (daily precipitation $\geq 1$ mm)	day
2	SDII	The amount of precipitation mean on wet days (daily precipitation $\geq 1$ mm)	mm.day <sup>-1</sup>
3	CDD	Maximum number of consecutive dry days (daily precipitation $< 1$ mm.day <sup>-1</sup> )	day
4	CWD	Maximum number of consecutive wet days (daily precipitation $\geq 1$ mm.day <sup>-1</sup> )	day
5	RX1day	The maximum one-day precipitation accumulation	mm
6	R95pTOT	Precipitation percent due to very heavy precipitation days.	%
Extreme temperature indices			
7	TXn	Minimum value of daily maximum temperature	°C
8	TXx	Maximum value of daily maximum temperature	°C
9	TNn	Minimum value of daily minimum temperature	°C
10	TNx	Maximum value of daily minimum temperature	°C

862

863 **Table1:** The 10 extreme climate indices used in this study.

864

865

866

867

		Central Sahel		West Sahel		Guinea coast		West Africa	
		MB	PCC	MB	PCC	MB	PCC	MB	PCC
R1mm	TRMM_2003	<b>-6.76</b>	0.98	-3.15	0.99	<b>8.89</b>	0.99	-1.12	<b>0.98</b>
	CTRL_2003	33.17	0.98	-5.25	0.96	<b>53.16</b>	0.96	22.18	<b>0.96</b>
	TRMM_2004	<b>-7.51</b>	0.98	-3.42	0.99	<b>10.44</b>	0.98	-1.34	<b>0.98</b>
	CTRL_2004	29.50	0.98	1.34	0.96	<b>55.46</b>	0.96	23.85	<b>0.95</b>
SDII	TRMM_2003	<b>2.67</b>	0.96	0.22	0.94	<b>-5.24</b>	0.95	1.20	<b>0.86</b>
	CTRL_2003	-7.52	0.97	-9.95	0.94	<b>-13.62</b>	0.77	-7.67	<b>0.73</b>
	TRMM_2004	<b>2.07</b>	0.96	0.45	0.96	<b>-6.44</b>	0.94	1.16	<b>0.86</b>
	CTRL_2004	-7.01	0.97	-9.37	0.94	<b>-14.65</b>	0.81	-7.59	<b>0.77</b>
CDD	TRMM_2003	1.21	0.95	0.89	0.93	-0.93	0.94	<b>-2.29</b>	<b>0.92</b>
	CTRL_2003	0.93	0.90	<b>14.49</b>	0.91	<b>-7.84</b>	0.66	<b>2.63</b>	<b>0.85</b>
	TRMM_2004	2	0.95	1.58	0.96	-3.17	0.92	<b>-1.75</b>	<b>0.94</b>
	CTRL_2004	4.75	0.91	<b>17.51</b>	0.95	<b>-9.43</b>	0.68	<b>6.99</b>	<b>0.89</b>
CWD	TRMM_2003	<b>-0.48</b>	0.92	0.80	0.94	<b>2.47</b>	0.92	0.37	<b>0.90</b>
	CTRL_2003	45.56	0.83	18.44	0.75	<b>59.21</b>	0.88	31.20	<b>0.81</b>
	TRMM_2004	<b>-0.68</b>	0.92	0.97	0.92	<b>2.38</b>	0.89	0.26	<b>0.87</b>
	CTRL_2004	36.78	0.79	20.48	0.78	<b>60.51</b>	0.82	29.74	<b>0.79</b>
RX1day	TRMM_2003	<b>35.78</b>	0.92	25.31	0.89	14.31	0.86	26.02	<b>0.84</b>
	CTRL_2003	-26.46	0.78	<b>-38.07</b>	0.91	<b>-30.28</b>	0.54	-20.08	<b>0.50</b>
	TRMM_2004	<b>31.66</b>	0.91	20.19	0.91	10	0.88	22.19	<b>0.85</b>
	CTRL_2004	-22.89	0.46	<b>-36.67</b>	0.88	<b>-42.44</b>	0.42	-20.23	<b>0.40</b>
R95pTOT	TRMM_2003	23.19	0.92	13.31	0.94	-0.23	0.96	<b>16.54</b>	<b>0.91</b>
	CTRL_2003	-27.67	0.67	-33.39	0.77	<b>-43.22</b>	0.65	-29.12	<b>0.59</b>
	TRMM_2004	23.26	0.91	12.32	0.94	-0.93	0.95	<b>18.54</b>	<b>0.91</b>
	CTRL_2004	-24.38	0.46	-31.75	0.80	<b>-46.61</b>	0.60	-27.45	<b>0.55</b>

869

870 **Table 2:** The pattern correlation coefficient (PCC) and the mean bias (MB) of R1mm (in  
871 day), SDII (in mm.day<sup>-1</sup>), CDD (in day), CWD (in day), RX1day (in mm) and R95pTOT (in  
872 %) indices for TRMM observation and their corresponding control experiments (initialized  
873 with initial soil moisture of ERA20C reanalysis) with respect to CHIRPS, calculated over  
874 Guinea coast, central Sahel, west Sahel and the entire West African domain for JJAS 2003  
875 and JJAS 2004.

876

		Central Sahel		West Sahel		guinea		West Africa	
		MB	PCC	MB	PCC	MB	PCC	MB	PCC
TXx	EIN_2003	<b>-2.17</b>	0.99	<b>-3.05</b>	0.99	<b>-4</b>	0.99	<b>-2.77</b>	<b>0.99</b>
	CTRL_2003	2.10	0.99	<b>3.02</b>	0.99	-1.34	0.99	0.32	<b>0.99</b>
	EIN_2004	<b>-2.44</b>	0.99	<b>-3.86</b>	0.99	<b>-3.84</b>	0.99	<b>-2.94</b>	<b>0.99</b>
	CTRL_2004	1.14	0.99	<b>2.02</b>	0.99	-1.41	0.99	-0.16	<b>0.99</b>
TXn	EIN_2003	0.31	0.99	<b>-1.48</b>	0.99	-0.70	0.99	0.50	<b>0.99</b>
	CTRL_2003	5.12	0.99	<b>6.56</b>	0.99	3.76	0.99	<b>5.65</b>	<b>0.99</b>
	EIN_2004	-0.76	0.99	<b>-1.73</b>	0.99	-1.38	0.99	-0.32	<b>0.99</b>
	CTRL_2004	3.43	0.99	<b>5.44</b>	0.99	2.75	0.99	<b>4.14</b>	<b>0.99</b>
TNn	EIN_2003	3.08	0.99	<b>3.43</b>	0.99	1.28	0.99	3.15	<b>0.99</b>
	CTRL_2003	2.37	0.99	<b>3.30</b>	0.99	1.53	0.99	1.45	<b>0.99</b>
	EIN_2004	3.28	0.99	<b>2.98</b>	0.99	1.20	0.99	3.11	<b>0.99</b>
	CTRL_2004	2.09	0.99	<b>2.55</b>	0.99	1.28	0.99	0.71	<b>0.99</b>
TNx	EIN_2003	-0.69	0.99	-1.79	0.99	<b>-3.11</b>	0.99	-1.62	<b>0.99</b>
	CTRL_2003	-1.91	0.99	-2.86	0.99	<b>-3.35</b>	0.99	-3.85	<b>0.99</b>
	EIN_2004	-0.82	0.99	-1.43	0.99	<b>-3.14</b>	0.99	-1.71	<b>0.99</b>
	CTRL_2004	-1.90	0.99	-2.54	0.99	<b>-3.32</b>	0.99	-3.99	<b>0.99</b>

878

879 **Table 3:** The pattern correlation coefficient (PCC) and the mean bias (MB in°C) of TXx,  
880 TXn, TNn and TNx indices from the EIN reanalysis and their corresponding control  
881 experiments (initialized with initial soil moisture of ERA20C reanalysis) with respect to GTS,  
882 calculated for Guinea coast, central Sahel, west Sahel and the entire West African domain for  
883 JJAS 2003 and JJAS 2004.

884

885

Precipitation indices		Central Sahel		West Sahel		Guinea coast		West Africa	
		$\Delta WC$	$\Delta DC$	$\Delta WC$	$\Delta DC$	$\Delta WC$	$\Delta DC$	$\Delta WC$	$\Delta DC$
R1mm (day)	2003	8.14	<b>-5.19</b>	<b>12.02</b>	0.69	3.92	2.88	4.67	1.75
	2004	10.01	-3.79	10.14	0.56	4.90	3.57	7.90	2.61
SDII (mm/day)	2003	0.07	0.11	-0.11	0.14	0.70	0.17	0.29	0.31
	2004	0.03	0.09	0.26	-0.07	0.56	0.22	0.24	0.21
CWD (day)	2003	13.25	-3.15	6.61	0.64	12.24	4.05	9.43	1.09
	2004	<b>15.58</b>	<b>-4.48</b>	7.20	-0.19	6.08	3.18	11.89	-0.37
CDD (day)	2003	-2.80	2.58	<b>-12.73</b>	0.83	-0.68	-1.31	-1.53	0.19
	2004	-5.92	<b>3.80</b>	-7.75	2.75	-0.93	-1.46	-3.57	-0.44
RX1day (mm)	2003	1.97	3.78	0.11	0.65	<b>26.14</b>	4.17	7.16	7.27
	2004	3.35	3.03	7.05	0.19	<b>14.93</b>	15.73	6.46	2.28
R95pTOT (%)	2003	1.54	1.77	2.88	1.53	<b>4.33</b>	2.37	2.83	2.46
	2004	1.66	0.89	<b>4.03</b>	0.43	1.69	0.92	1.37	2.43

886

887 **Table 4:** Summary Table of maximum values of change on PDF's for R1mm, SDII, CDD,  
888 CWD, RX-1day and R95pTOT indices.

889

890

891

892

893

894

895

896

897

898

899

900

901

902

903

904

905

Temperature indices		Central Sahel		West Sahel		Guinea coast		West Africa	
		$\Delta WC$	$\Delta DC$	$\Delta WC$	$\Delta DC$	$\Delta WC$	$\Delta DC$	$\Delta WC$	$\Delta DC$
TXx	2003	-2.54	1.14	-2.11	0.90	-0.34	0.68	-0.89	1.06
	2004	<b>-2.57</b>	<b>1.69</b>	-1.58	0.98	-0.32	1.01	-0.86	1.27
TXn	2003	-1.37	0.81	<b>-1.67</b>	-0.05	-0.06	0.28	-0.50	0.59
	2004	-1.09	<b>1.03</b>	-0.93	0.55	-0.04	0.31	-0.38	0.61
TNn	2003	-0.37	-0.20	-0.23	<b>-1.15</b>	0.05	0.04	-0.20	0.03
	2004	-0.03	-0.37	0.06	-1.07	<b>0.11</b>	-0.03	-0.05	-0.11
TNx	2003	-1.29	<b>0.25</b>	-0.94	-1.37	0.12	0.04	-0.49	0.13
	2004	<b>-1.67</b>	0.15	-0.62	-1.13	0.02	0.03	-0.51	-0.07

906

907 **Table 5:** Summary Table of maximum values of change on PDF's for TXx, TXn, TNn and  
 908 TNx indices.

909

910

911

912

913

914

915

916

917

918

919

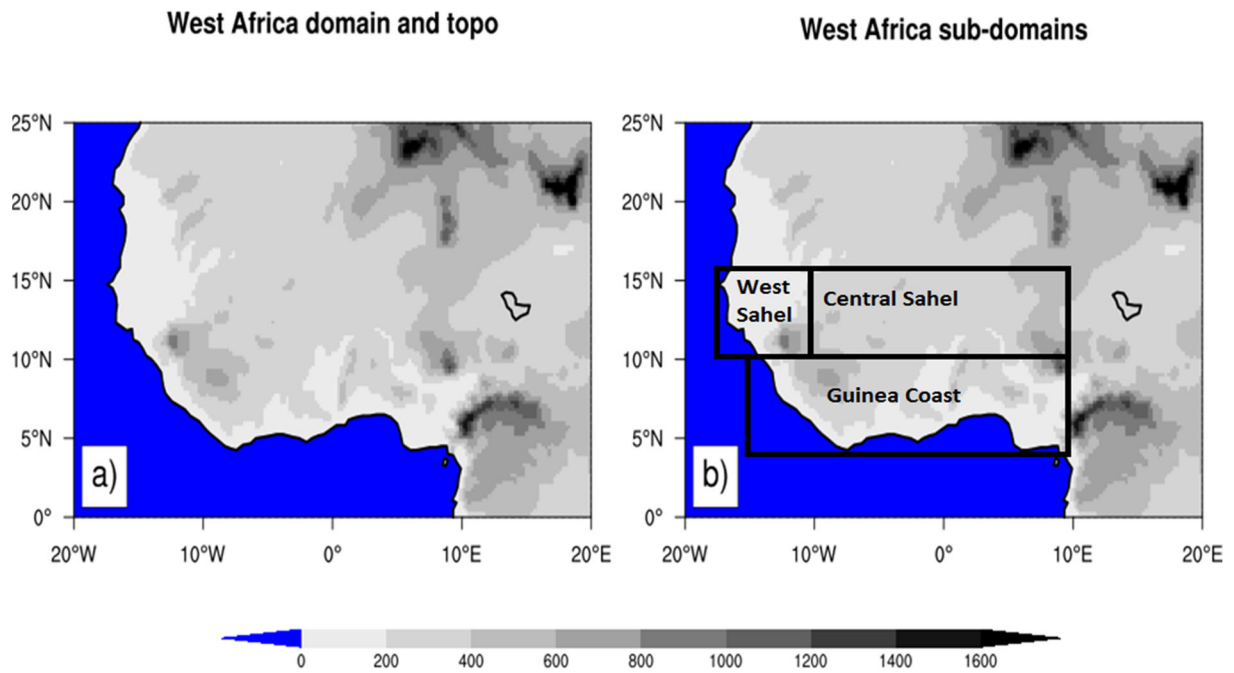
920

921

922

923

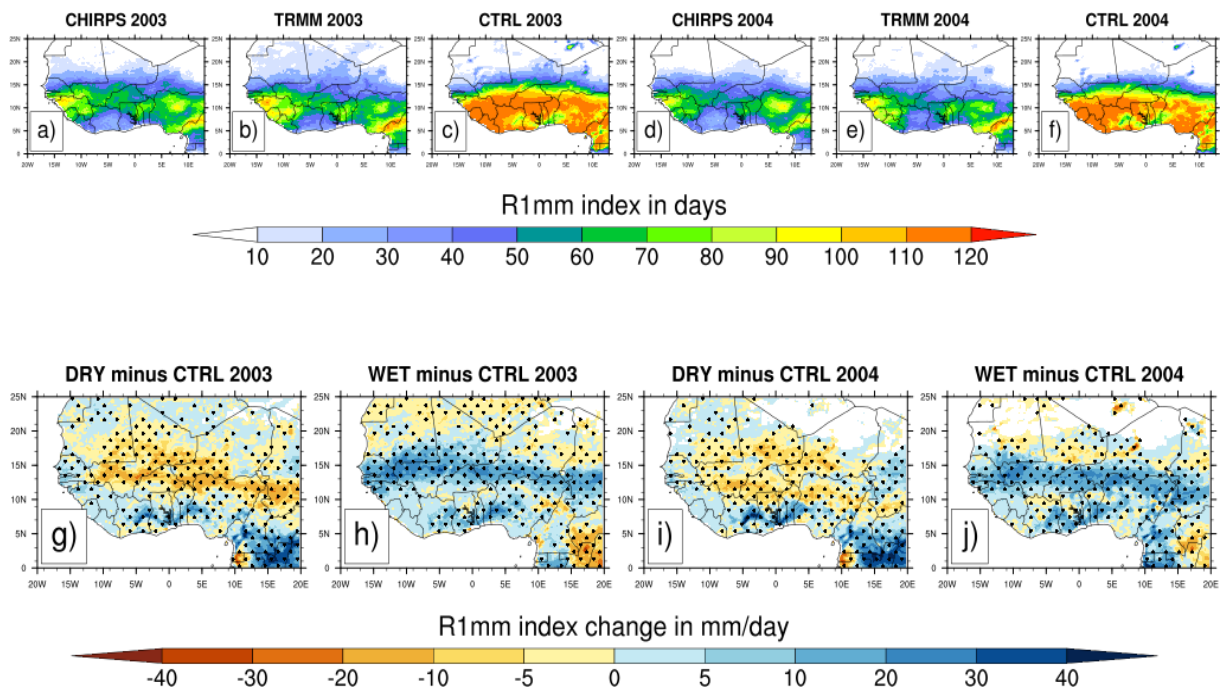




924  
925

926 **Figure 1:** Topography of the West African domain. The analysis of the model result has an  
927 emphasis on the whole West African domain and the three subregions Guinea coast, central  
928 Sahel and west Sahel, which are marked with black boxes.

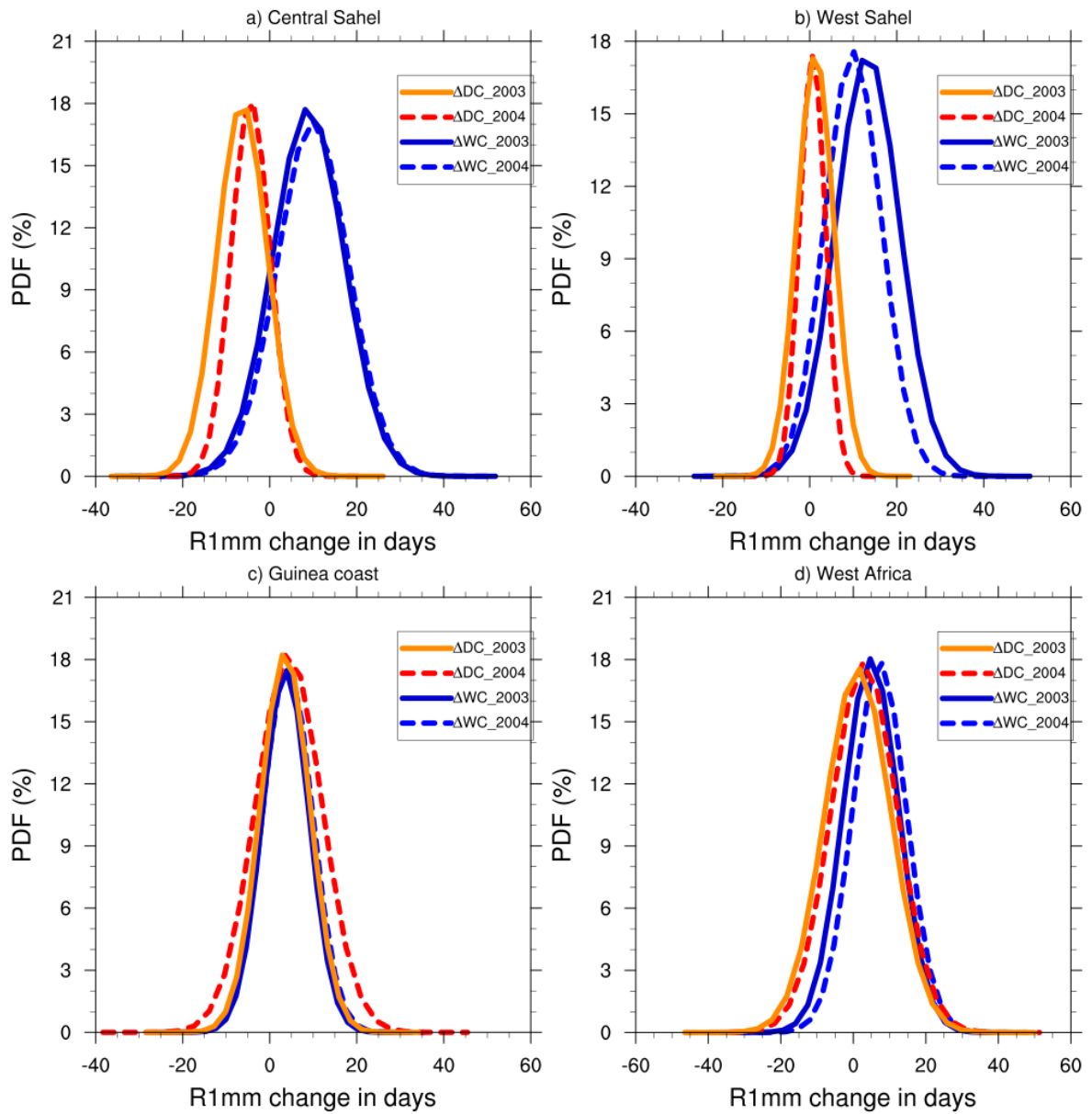
929  
930  
931  
932  
933  
934  
935  
936  
937  
938  
939  
940  
941  
942  
943  
944  
945



946  
947

948 **Figure2:** Mean values of the number of the wet days (R1mm index in days) from CHIRPS (a  
949 and d) and TRMM(b and e) observations for JJAS 2003 and JJAS 2004 and their  
950 corresponding simulated control (CTRL) experiments (c and f) initialized with initial soil  
951 moisture of the reanalysis of ERA20C (first panel) and changes in R1mm index in days  
952 (second panel) for JJAS 2003 and JJAS 2004, from dry (g and i) and wet (h and j)  
953 experiments with respect to the corresponding control experiments. Areas with values  
954 passing the 10% significance test are dotted.

955  
956  
957  
958  
959  
960  
961  
962  
963  
964  
965



966

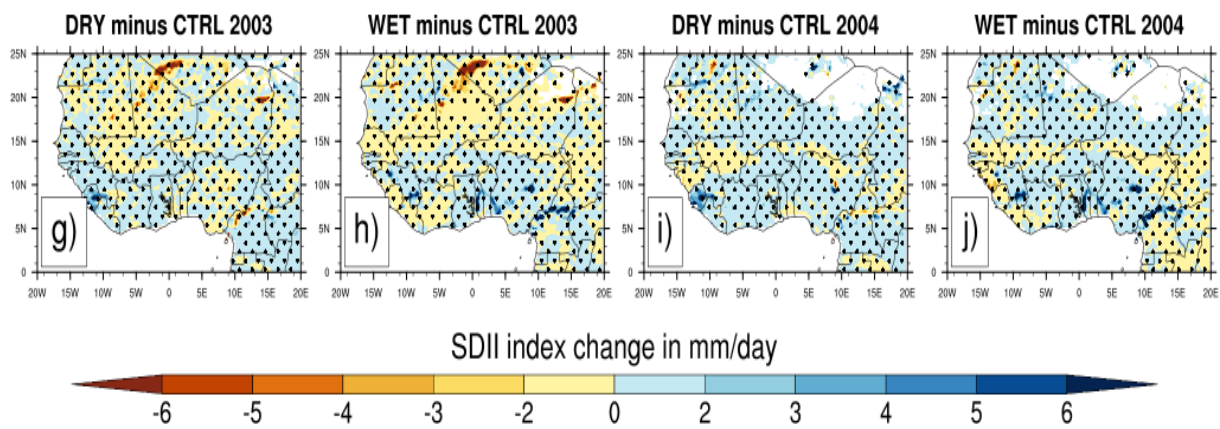
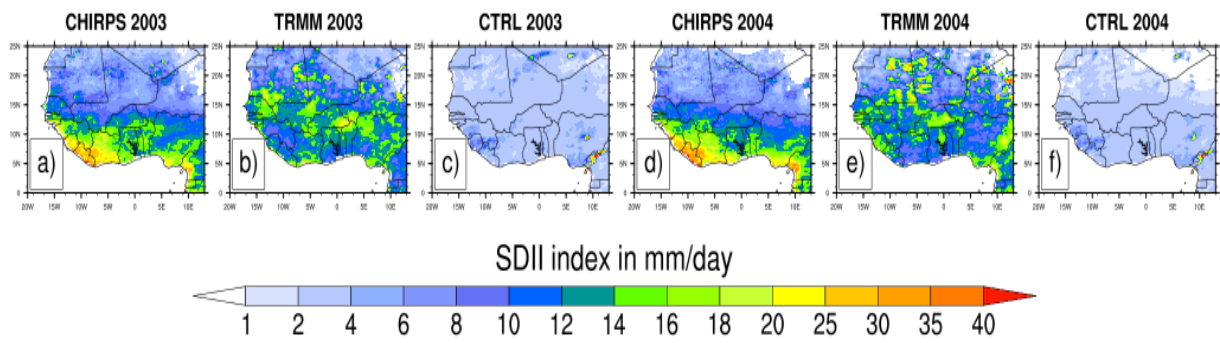
967

968 **Figure3:** PDF distributions (%) of mean values of the number of the wet days change in JJAS  
 969 2003 and JJAS 2004, over (a) central Sahel , (b) West Sahel, (c) Guinea and (d) West Africa  
 970 derived from dry ( $\Delta DC$ ) and wet ( $\Delta WC$ ) experiments with respect to their corresponding  
 971 control experiment.

972

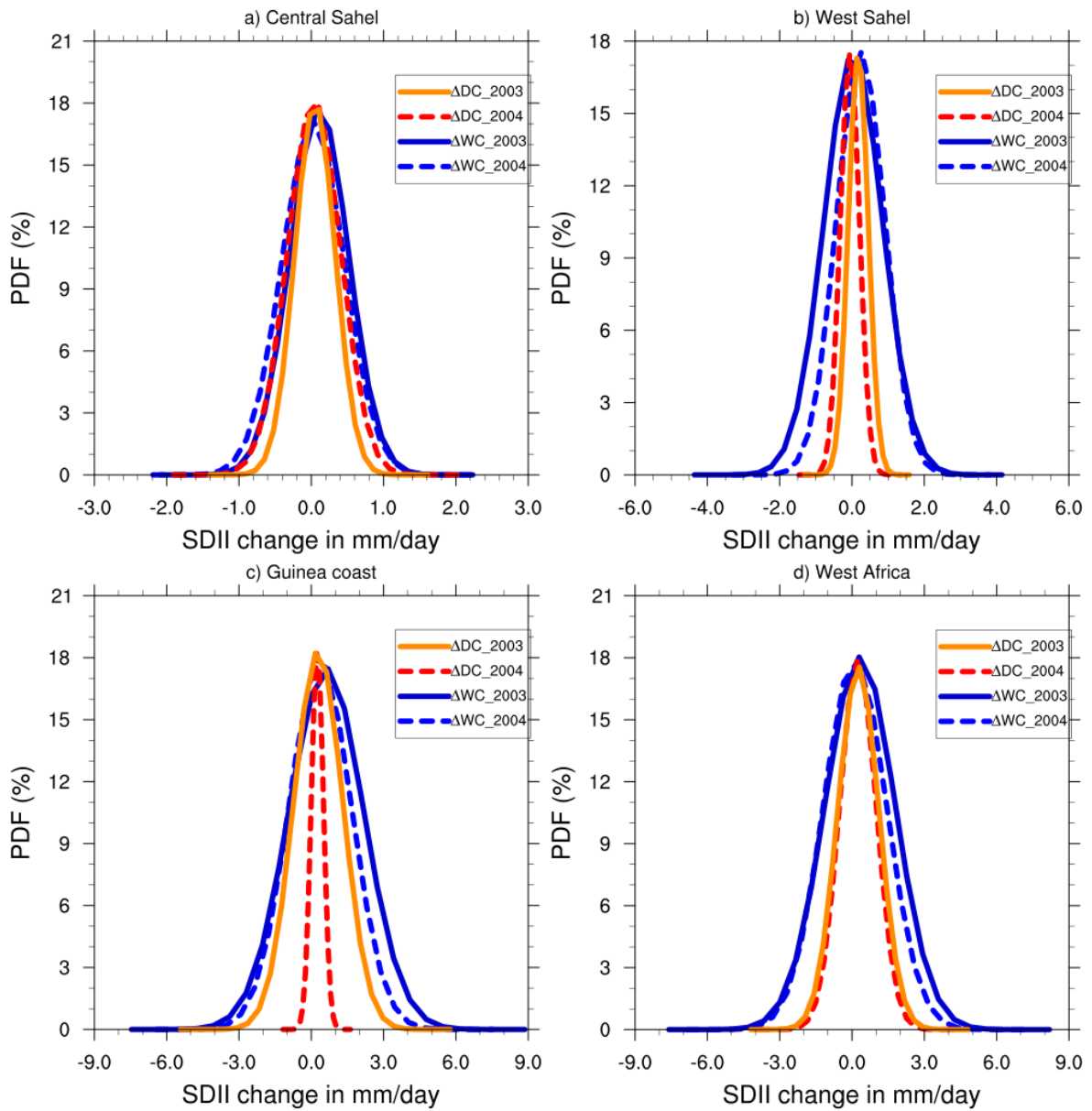
973

974



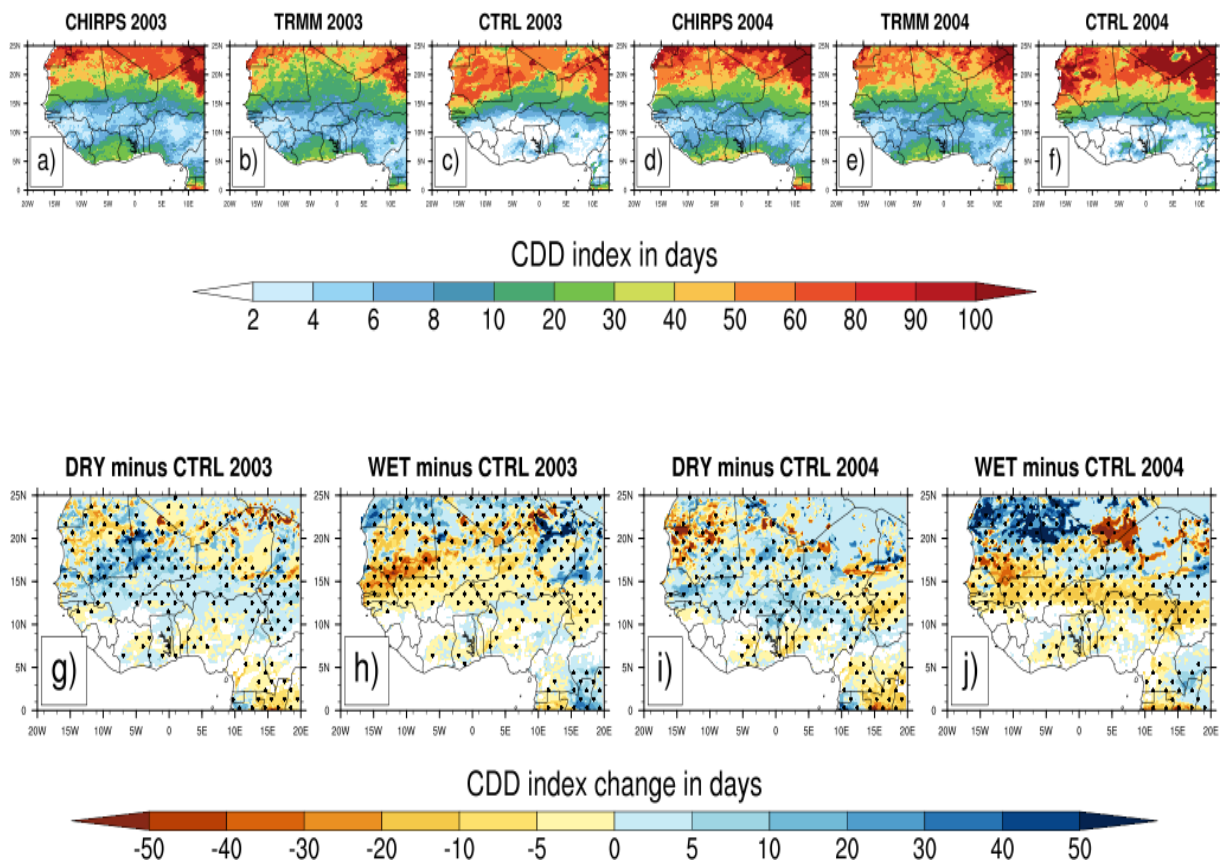
975  
976  
977  
978  
979  
980  
981  
982  
983  
984  
985  
986  
987  
988  
989  
990  
991

**Figure4:** Same as Fig. 2 but for the SDII index (in mm.day<sup>-1</sup>).



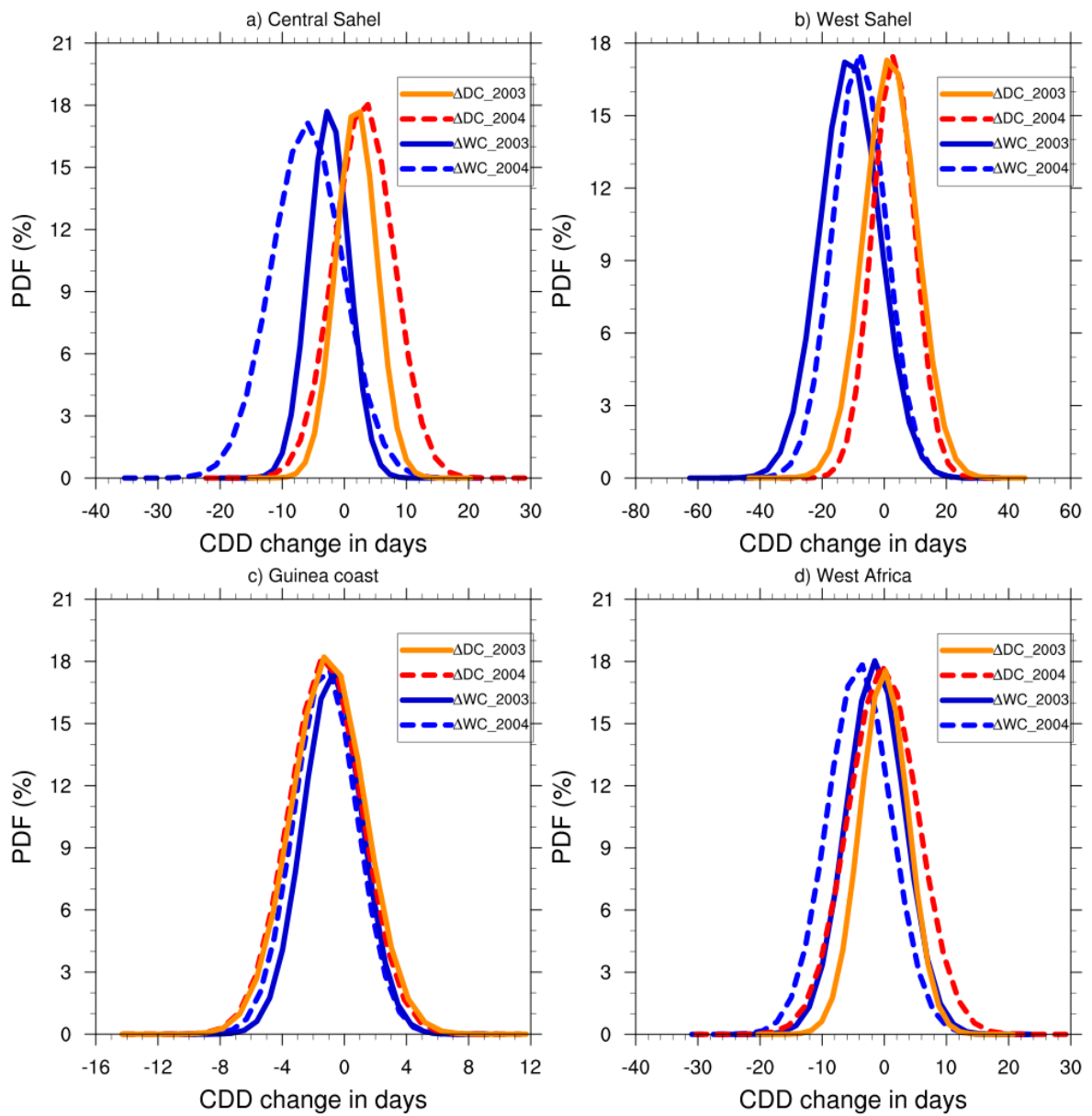
992  
 993  
 994  
 995  
 996  
 997  
 998  
 999  
 1000  
 1001  
 1002  
 1003

**Figure 5:** Same as Fig. 3 but for the SDII index (in mm.day<sup>-1</sup>).



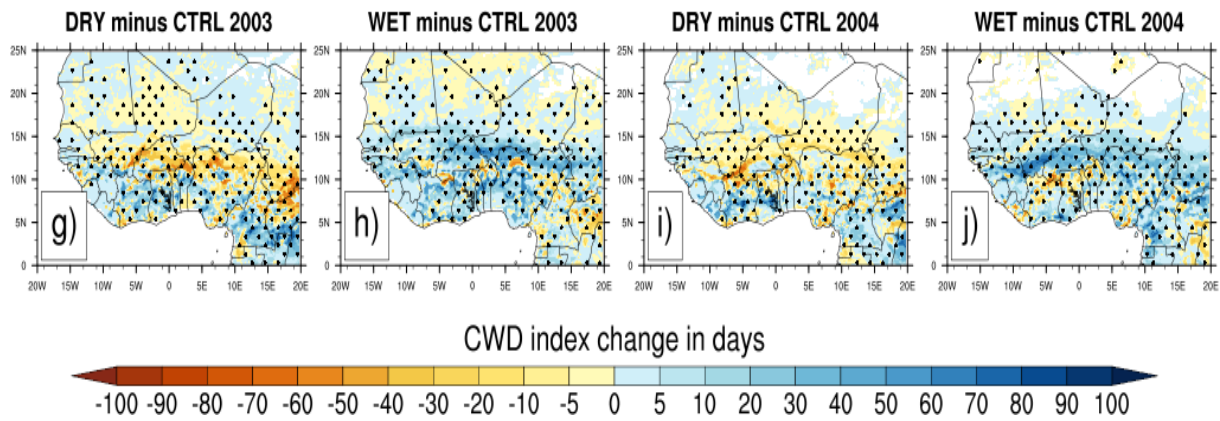
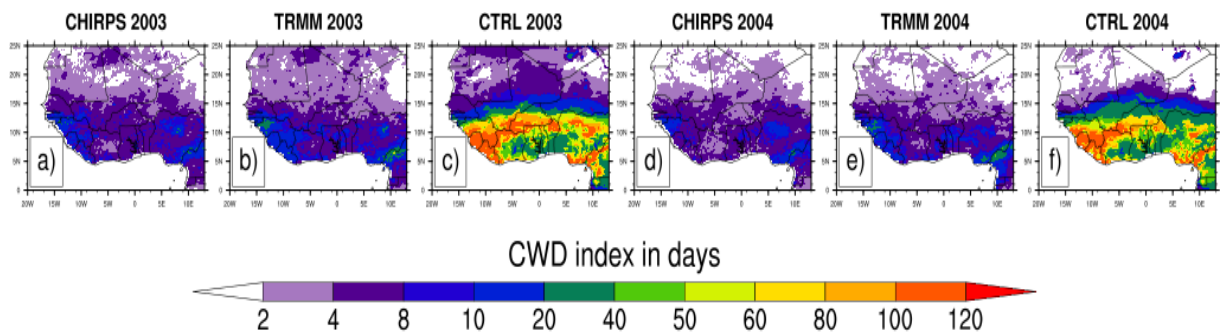
1004  
 1005  
 1006  
 1007  
 1008  
 1009  
 1010  
 1011  
 1012  
 1013  
 1014  
 1015  
 1016  
 1017  
 1018  
 1019  
 1020

**Figure 6:** Same as Fig. 2 but for the CDD index (in day).



1021  
 1022  
 1023  
 1024  
 1025  
 1026  
 1027  
 1028  
 1029  
 1030  
 1031

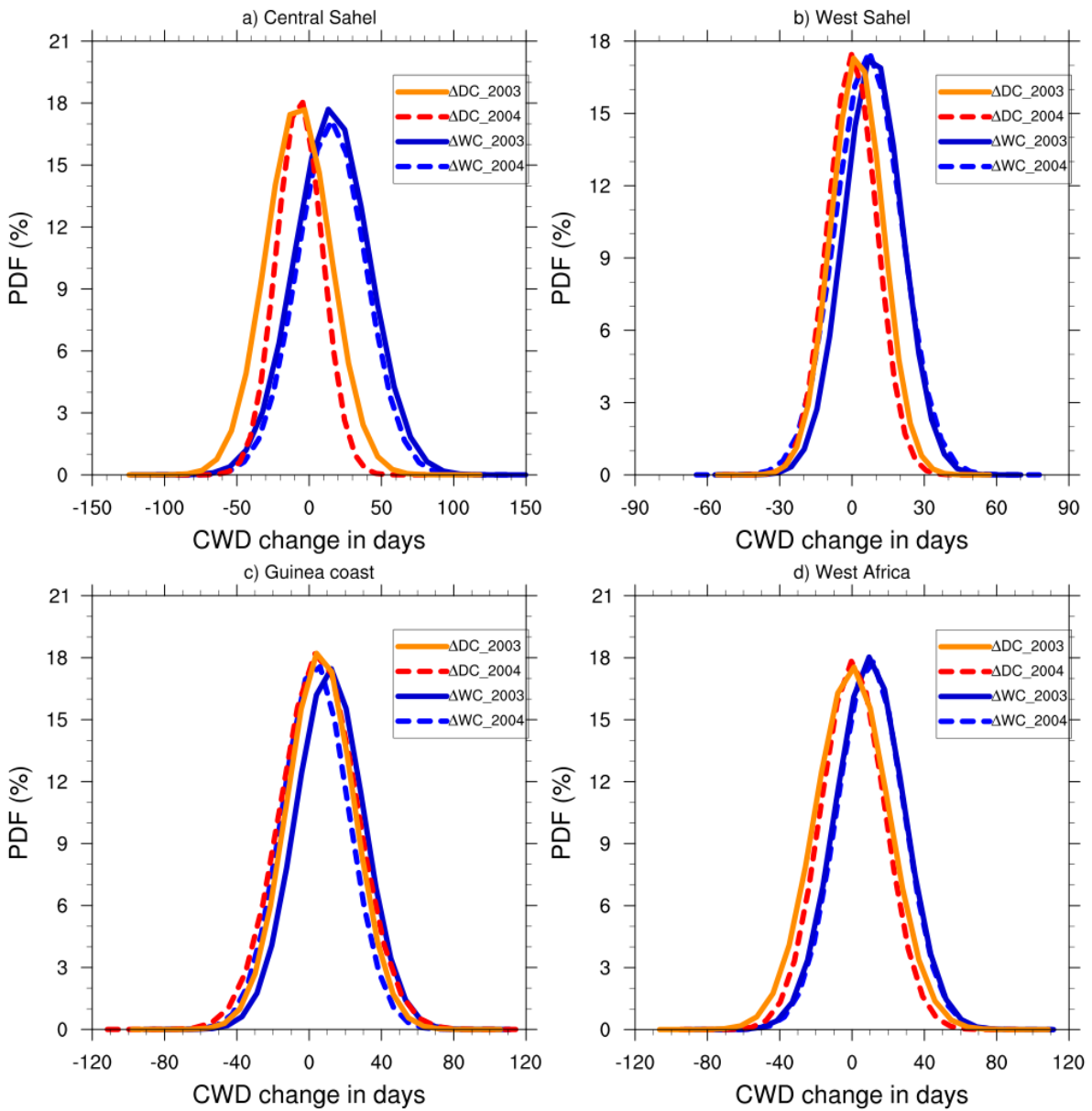
**Figure 7:** Same as Fig. 3 but for the CDD index (in day).



1032  
 1033  
 1034  
 1035  
 1036  
 1037  
 1038  
 1039  
 1040  
 1041  
 1042  
 1043  
 1044  
 1045  
 1046  
 1047  
 1048  
 1049  
 1050

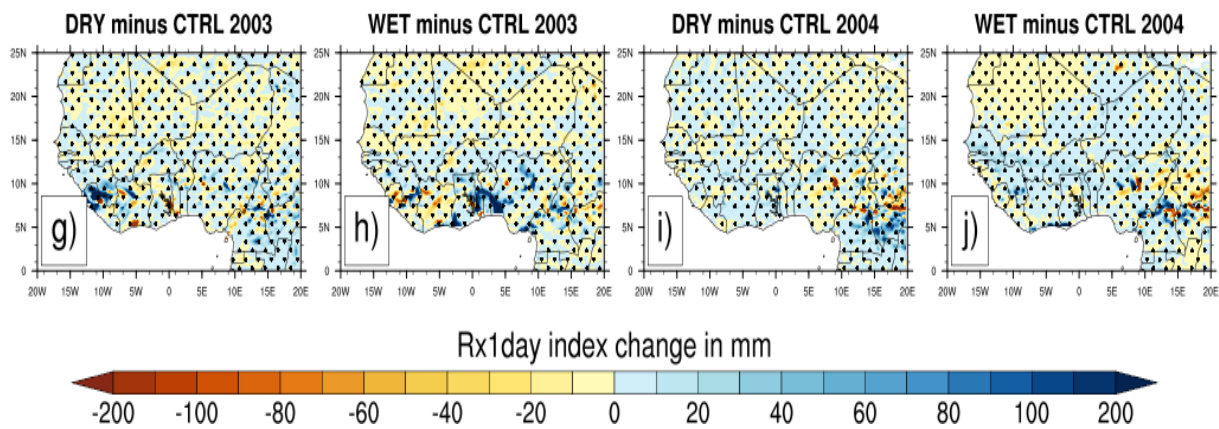
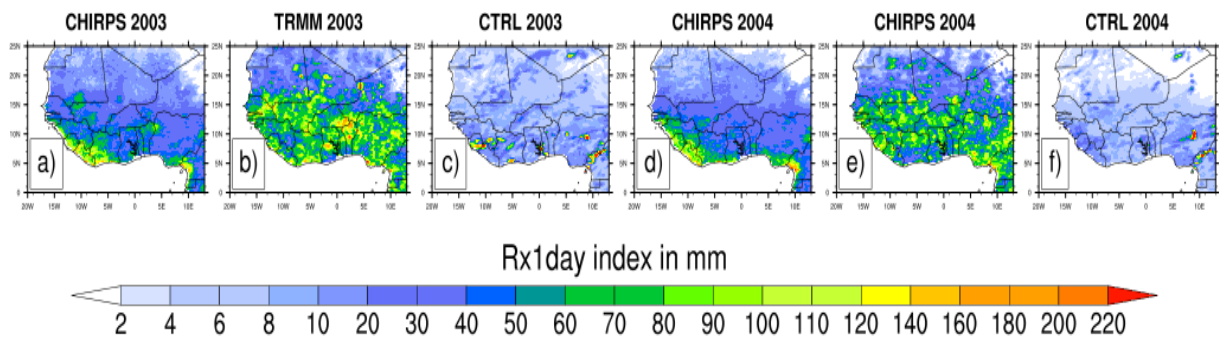
**Figure 8:** Same as Fig. 2 but for the CWD index (in day).





1051  
 1052  
 1053  
 1054  
 1055  
 1056  
 1057  
 1058  
 1059  
 1060  
 1061  
 1062

**Figure 9:** Same as Fig. 3 but for the CWD index (in day).



1063

1064

1065 **Figure 10:** Same as Fig. 2 but for the RX1day index (in mm).

1066

1067

1068

1069

1070

1071

1072

1073

1074

1075

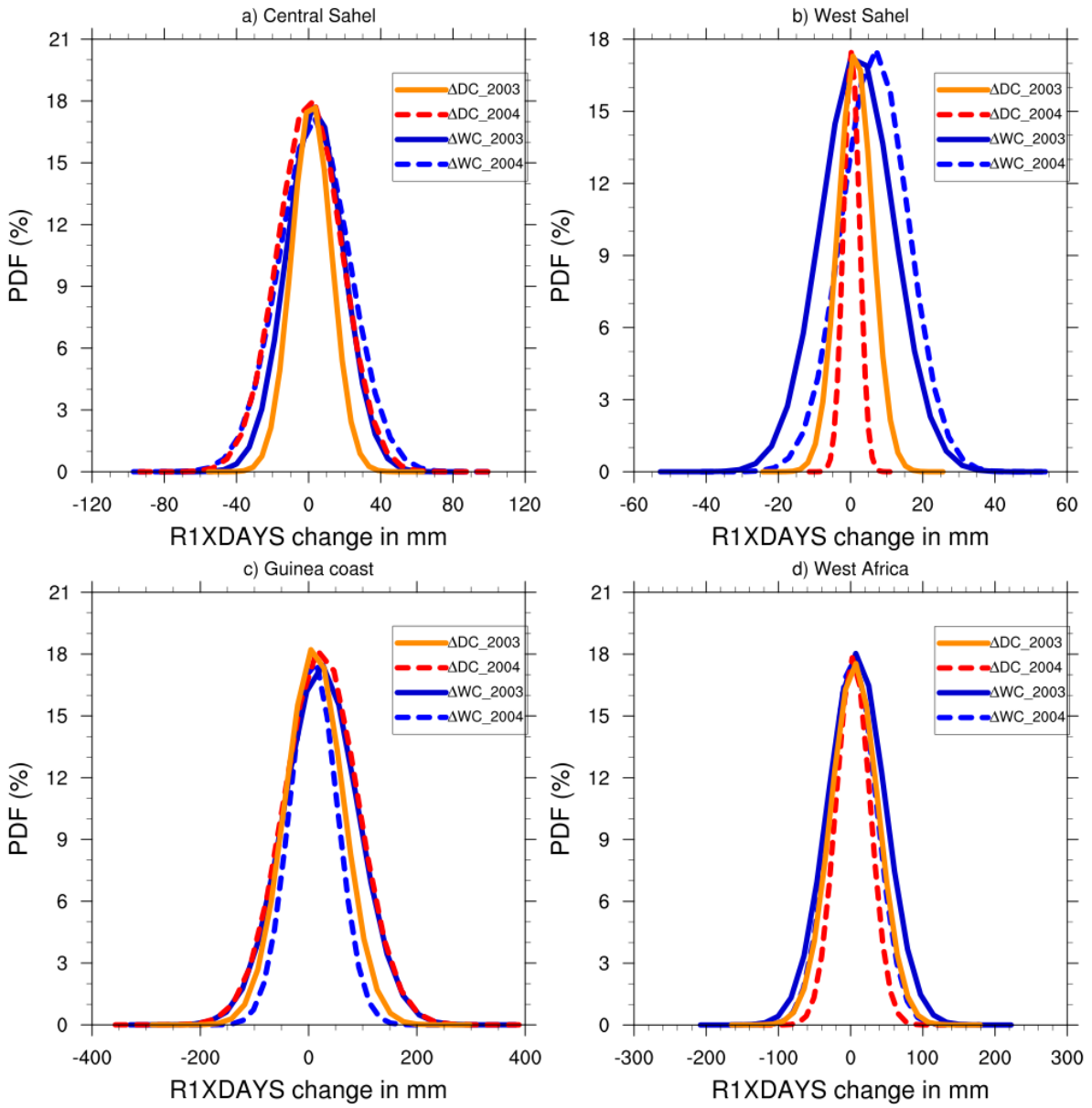
1076

1077

1078

1079

1080



1081

1082

1083

1084 **Figure 11:** Same as Fig. 3 but for the RX1DAY index (in mm).

1085

1086

1087

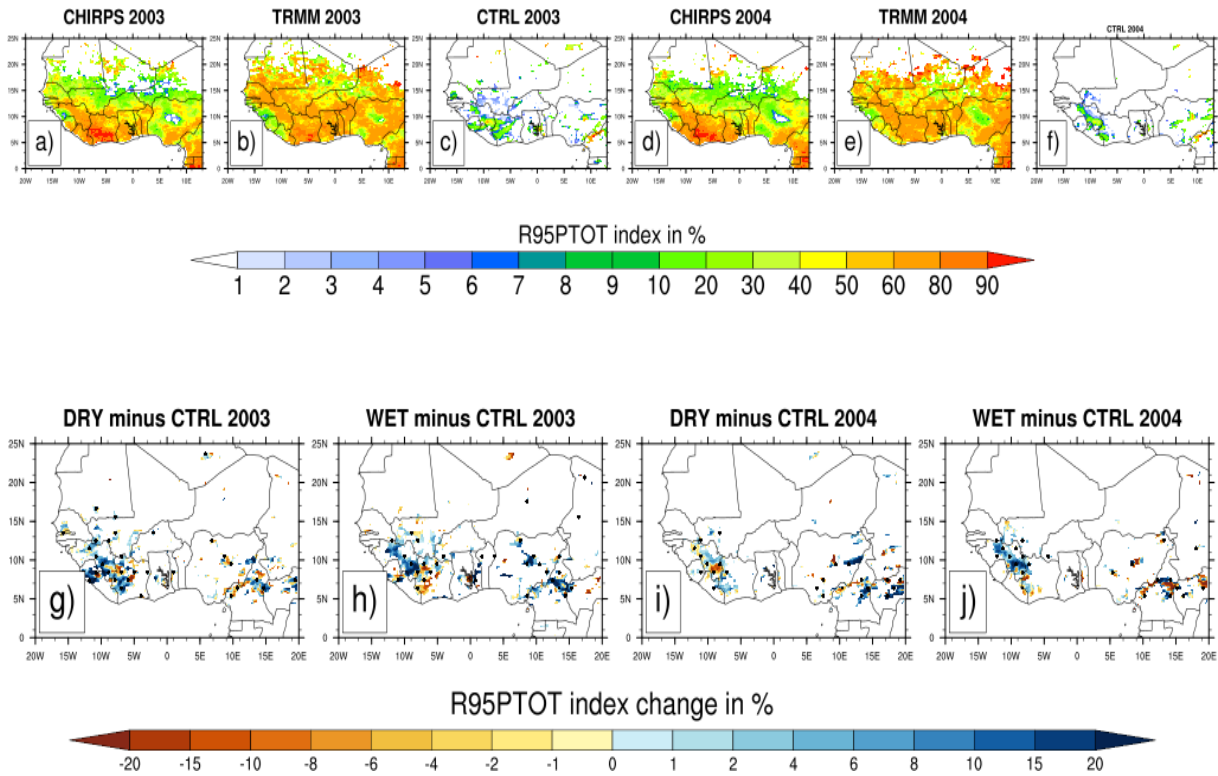
1088

1089

1090

1091

1092



1093

1094

1095 **Figure 12:** Same as Fig. 2 but for the R95pTOT index (in %).

1096

1097

1098

1099

1100

1101

1102

1103

1104

1105

1106

1107

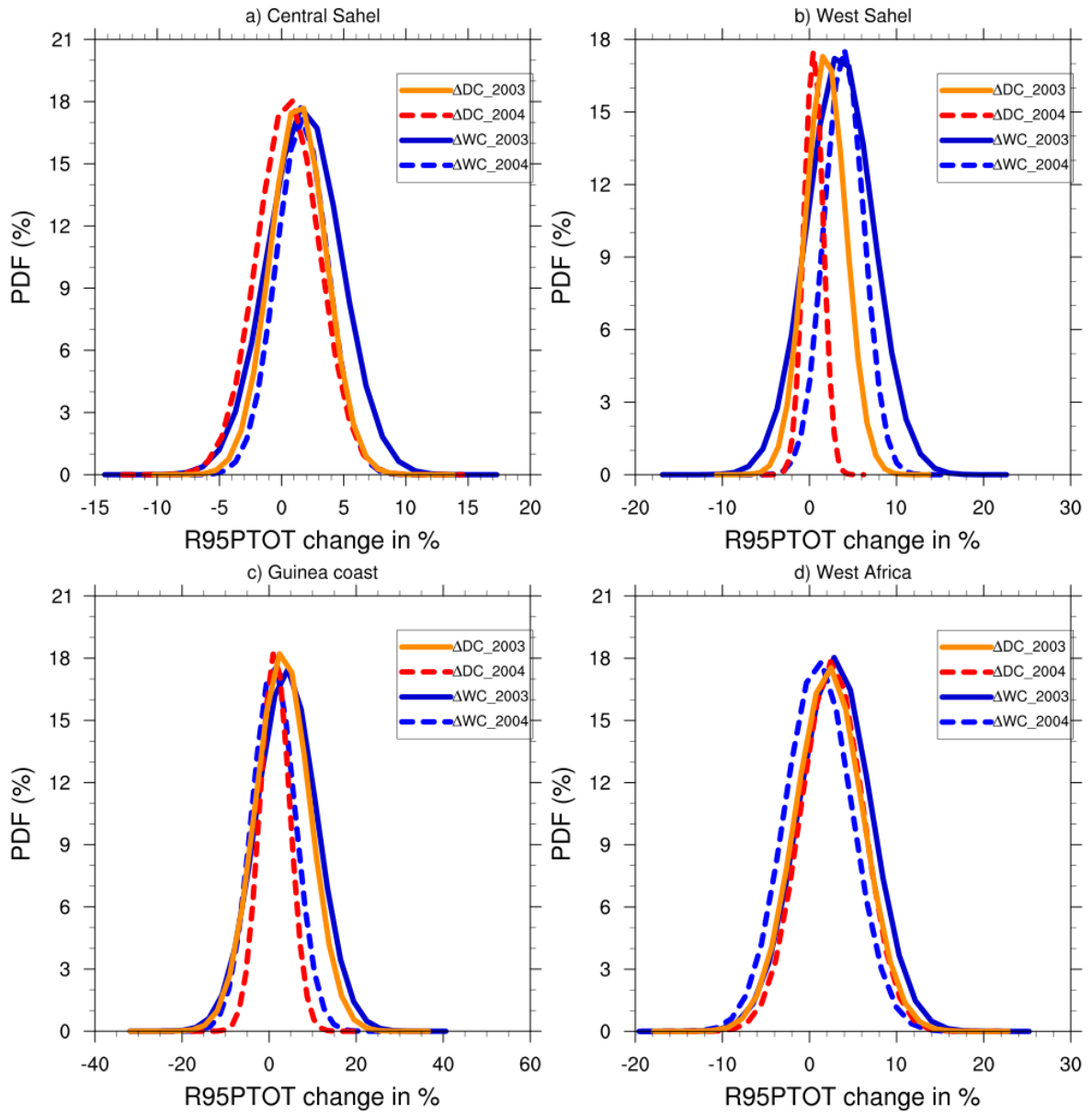
1108

1109

1110

1111

1112



1113

1114 **Figure 13:** Same as Fig. 3 but for the R95pT0T index (in %).

1115

1116

1117

1118

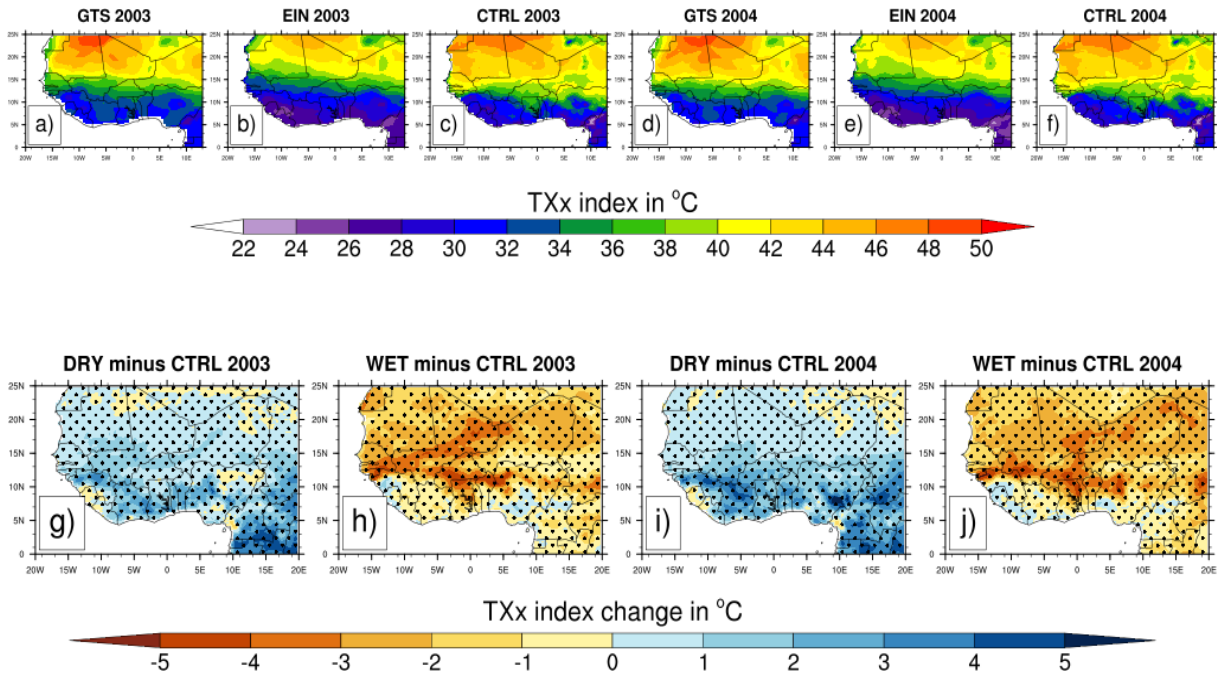
1119

1120

1121

1122

1123



1124

1125 **Figure 14:** The mean maximum value of daily maximum temperature (TXx index in °C) from  
1126 GTS observation (a and d) and The EIN reanalysis (b and e) for JJAS 2003 and JJAS 2004  
1127 and their corresponding simulated control (CTRL) experiments (c and f) initialized with the  
1128 initial soil moisture of the ERA20C reanalysis (first panel) and changes in TXx index in °C  
1129 (second panel) for JJAS 2003 and JJAS 2004, from dry (g and i) and wet (h and j)  
1130 experiments with respect to the corresponding control experiments. Areas with values passing  
1131 the 10% significance test are dotted.

1132

1133

1134

1135

1136

1137

1138

1139

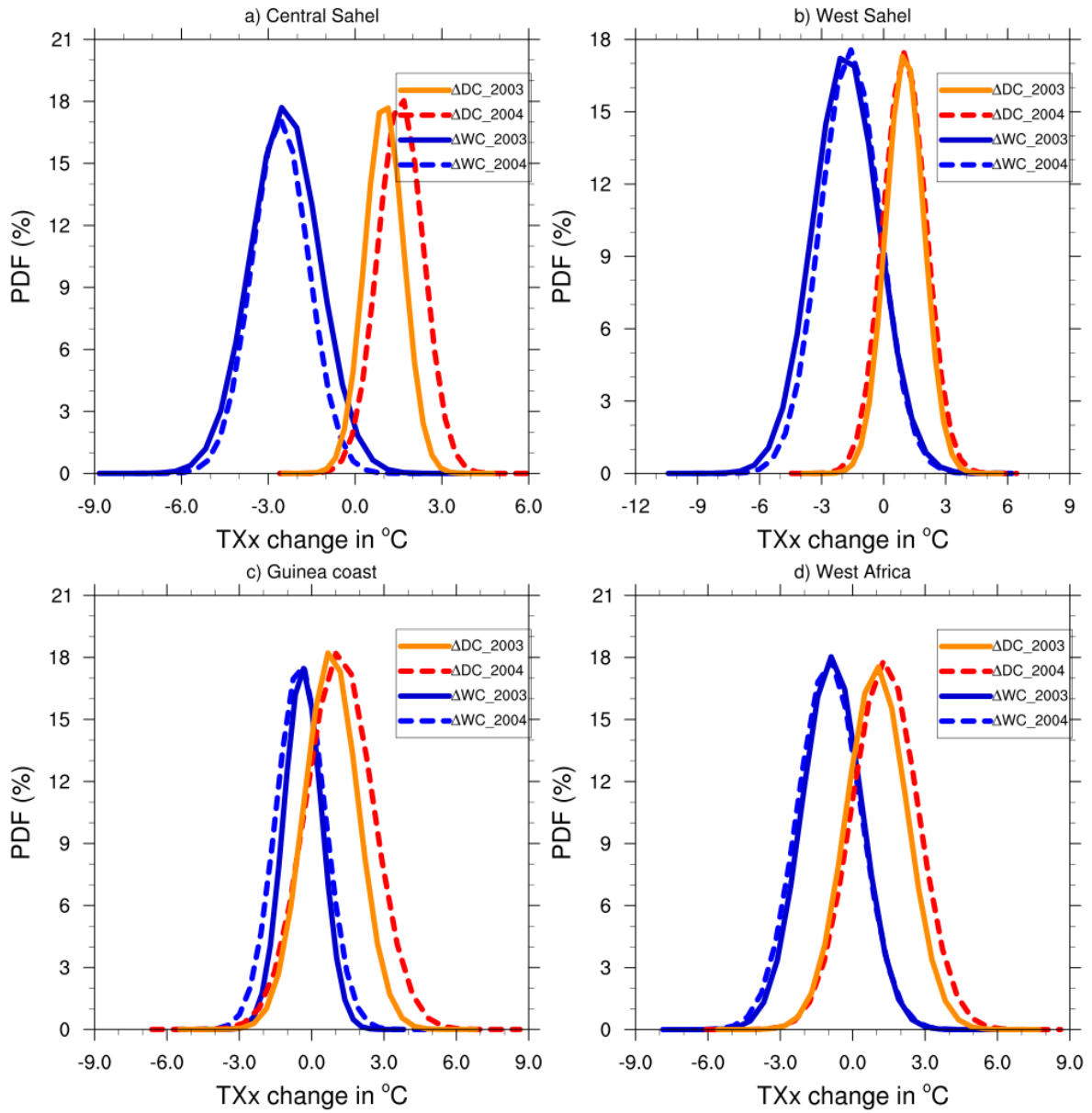
1140

1141

1142

1143

1144



1146

1147

1148 **Figure 15:** PDF distributions (%) of change in maximum value of daily maximum

1149 temperature (TXx index, in°C) for JJAS 2003 and JJAS 2004, over (a) central Sahel , (b)

1150 West Sahel, (c) Guinea and (d) West Africa derived from dry ( $\Delta DC$ ) and wet ( $\Delta WC$ )

1151 experiments compared to their corresponding control experiment.

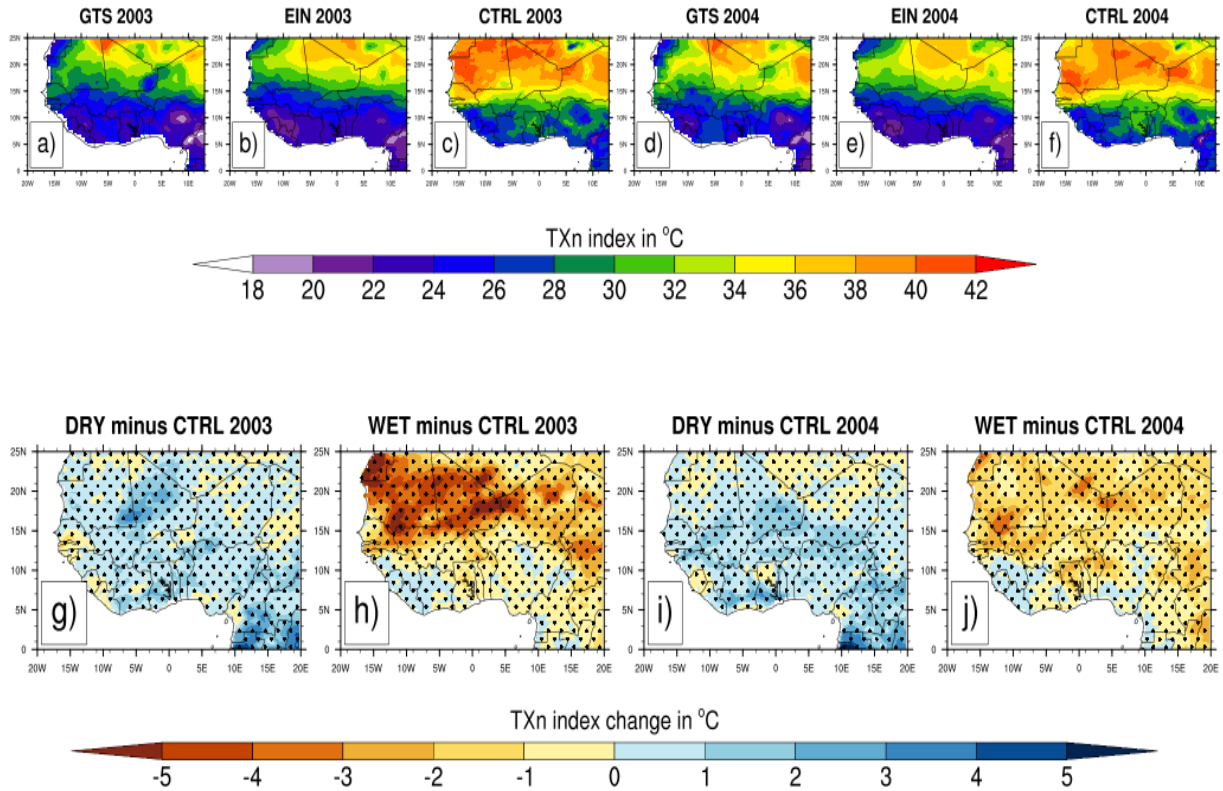
1152

1153

1154

1155

1156



1157

1158

1159

1160 **Figure 16:** Same as Fig. 14 but for the TXn index

1161

1162

1163

1164

1165

1166

1167

1168

1169

1170

1171

1172

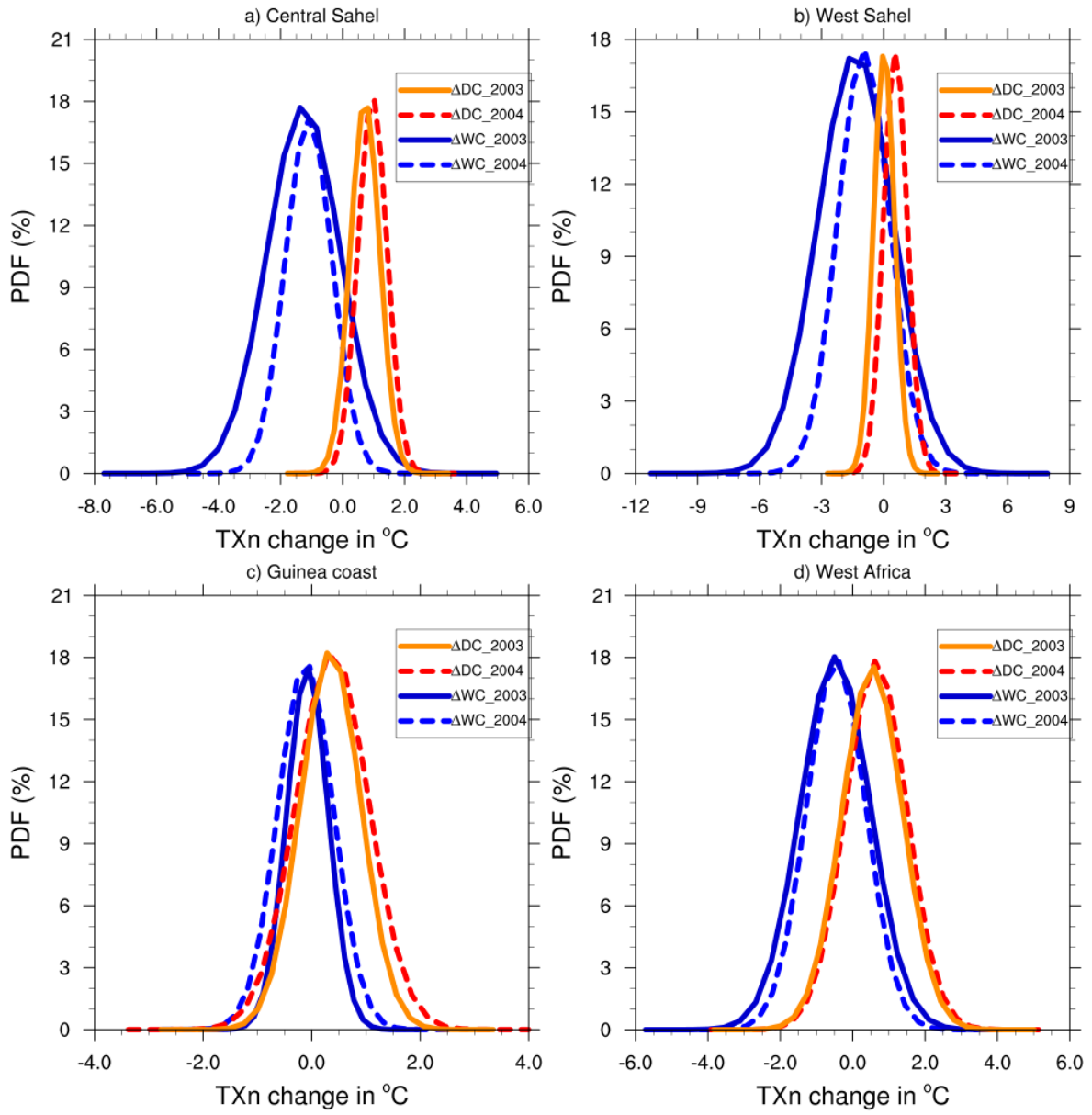
1173

1174

1175



1176



1177

1178

1179

1180

1181 **Figure 17:** Same as Fig. 15 but for the TXn index.

1182

1183

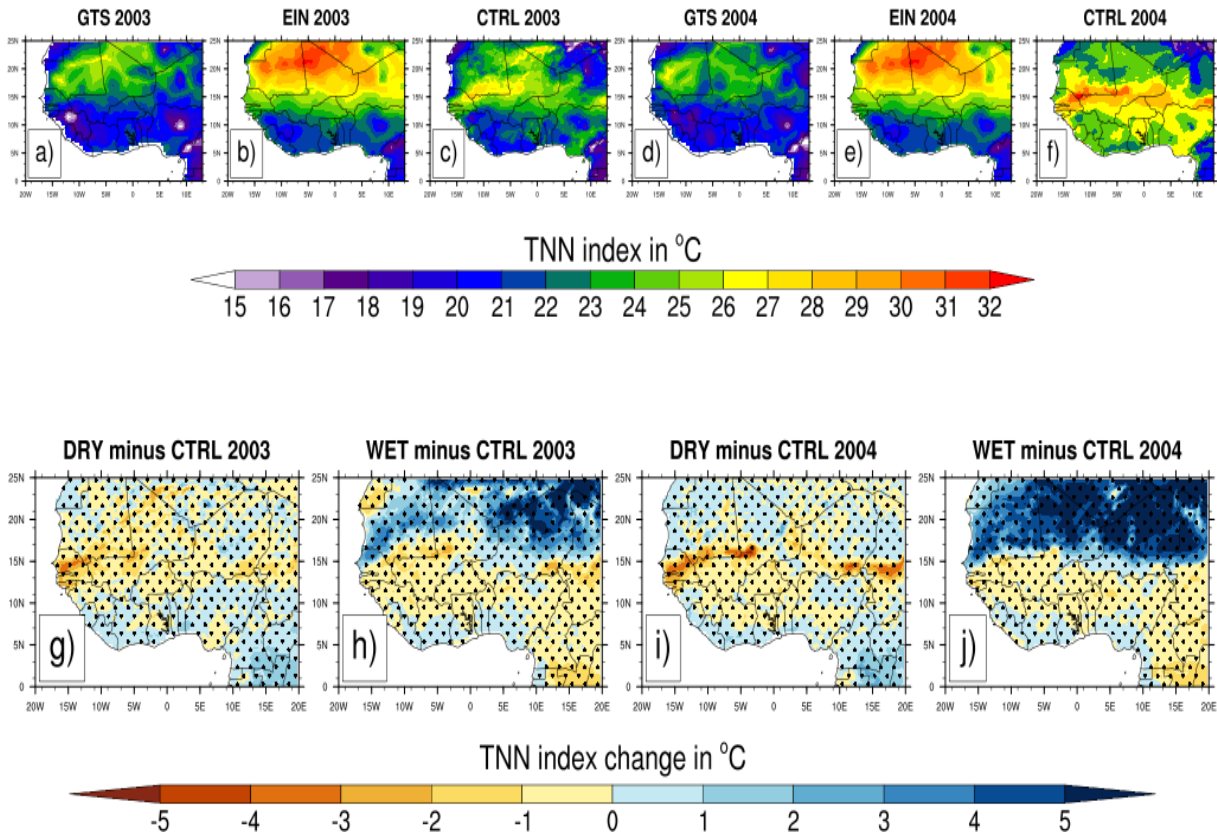
1184

1185

1186

1187

1188



1189

1190

1191

1192 **Figure 18:** Same as Fig. 14 but for the TNN index.

1193

1194

1195

1196

1197

1198

1199

1200

1201

1202

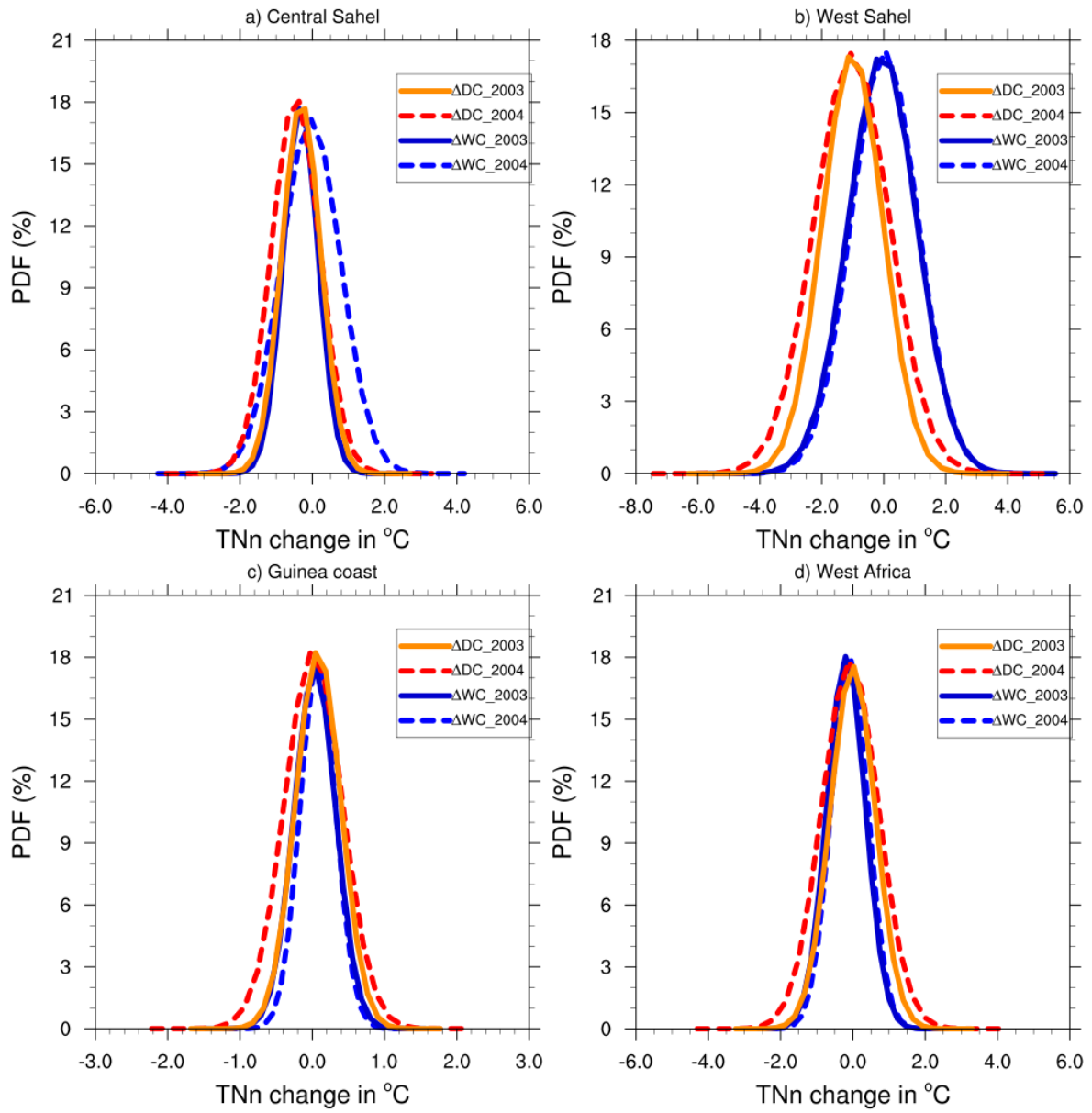
1203

1204

1205

1206

1207



1208

1209

1210

1211

1212 **Figure 19:** Same as Fig. 14 but for the TNn index.

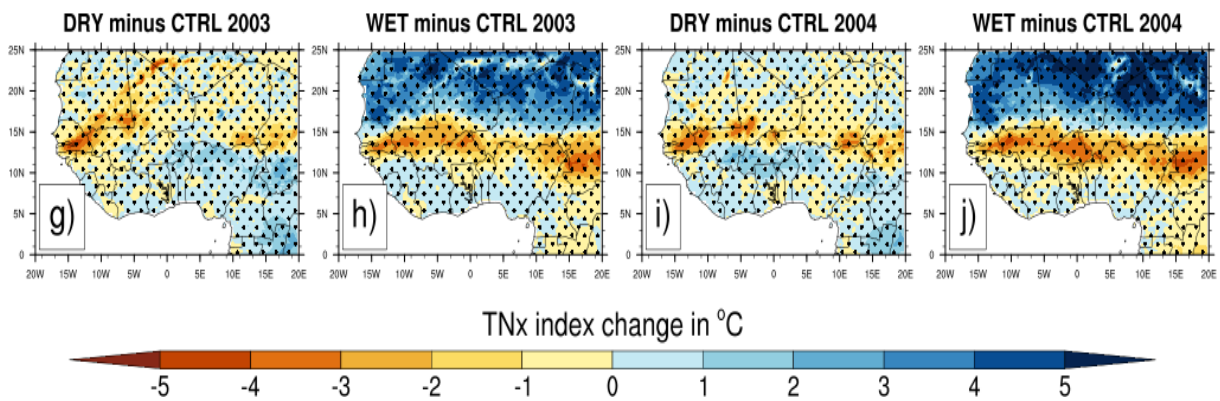
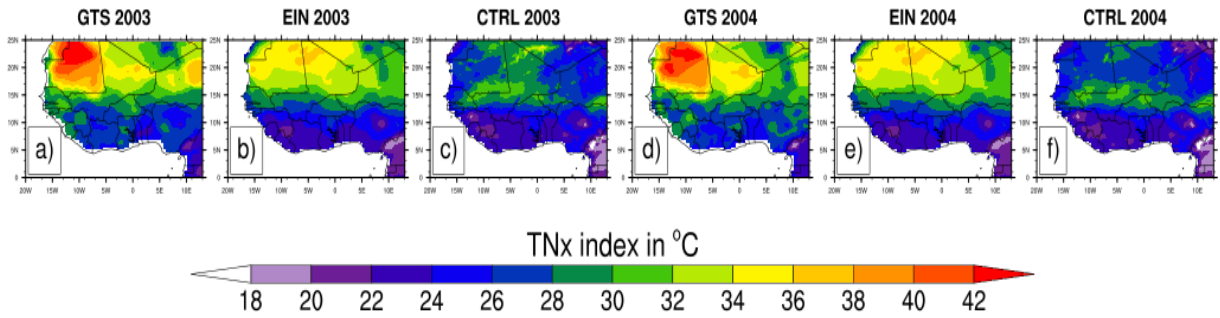
1213

1214

1215

1216

1217



1218

1219

1220 **Figure 20:** Same as Fig. 14 but for the TNx index

1221

1222

1223

1224

1225

1226

1227

1228

1229

1230

1231

1232

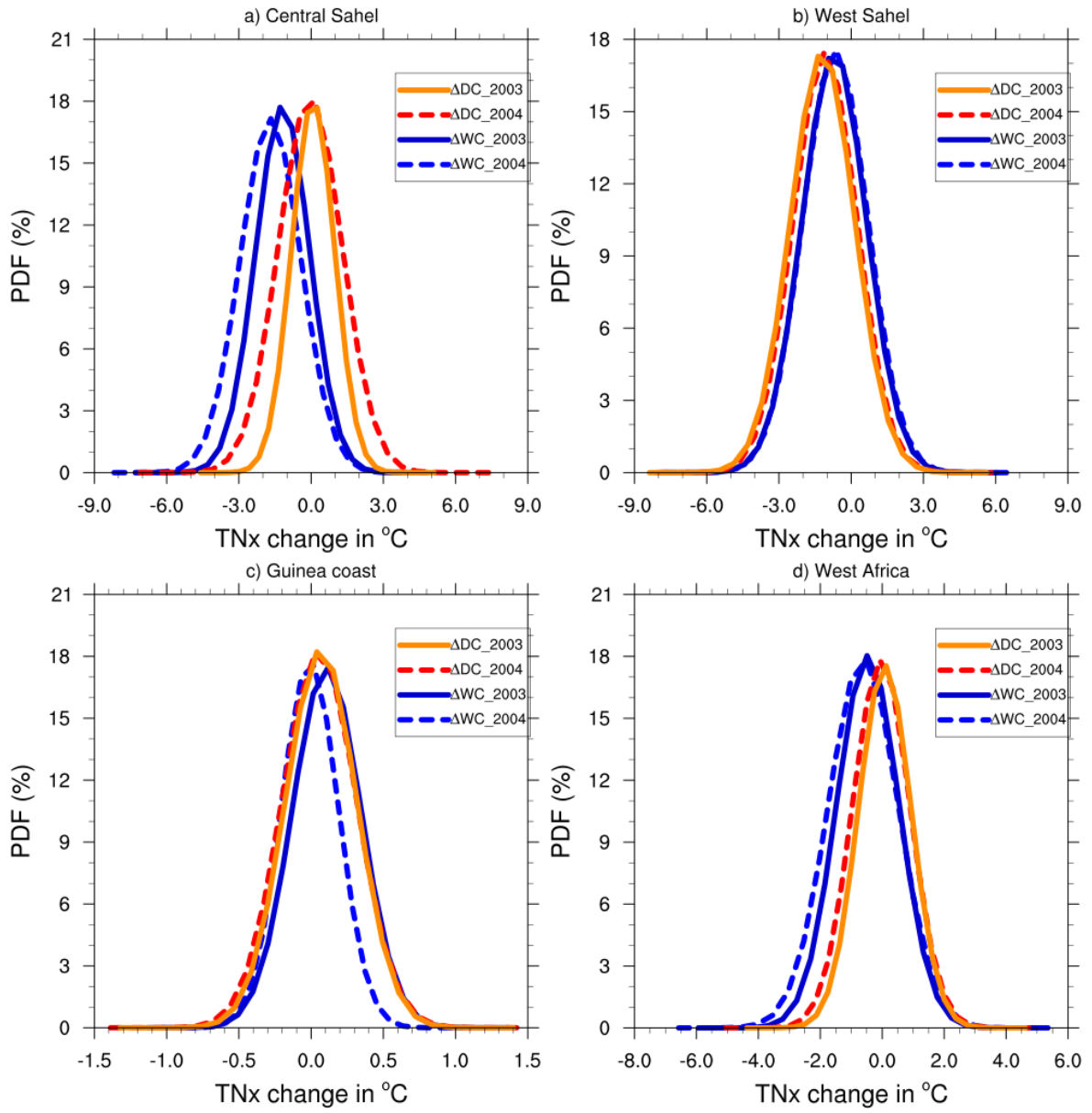
1233

1234

1235

1236

1237



1238

1239

1240 **Figure 21:** Same as Fig. 15 but for the TNx index.

1241

1242

1243